THE JOURNAL OF PHYSICAL CHEMISTRY B

ARTICLE

pubs.acs.org/JPCB

What Are the Differences between Ascorbic Acid and NADH as Hydride and Electron Sources in Vivo on Thermodynamics, Kinetics, and Mechanism?

Xiao-Qing Zhu,* Yuan-Yuan Mu, and Xiu-Tao Li

State Key Laboratory of Elemento-Organic Chemistry, Department of Chemistry, Nankai University, Tianjin 300071, China

ABSTRACT: Ascorbic acid ($AscH_2$) and dihydronicotinamide adenine dinucleotide (NADH) are two very important natural redox cofactors, which can be used as hydride, electron, and hydrogen atom sources to take part in many important bioreduction processes in vivo. The differences of the two natural reducing agents as hydride, hydrogen atom, and electron donors in thermodynamics, kinetics, and mechanisms were examined by using 5,6-isopropylidene ascorbate ($iAscH^-$) and β-D-glucopyranosyl-1,4-dihydronicotinamide acetate (GluNAH) as their models, respectively. The results show that the hydride-donating ability of $iAscH^-$ is smaller than that of GluNAH by 6.0 kcal/mol, but the electron-donating ability and hydrogen-donating ability of $iAscH^-$ are larger than those of GluNAH by 20.8 and 8.4 kcal/mol, respectively, which indicates that $iAscH^-$ is a good electron donor and a good hydrogen atom donor, but GluNAH is a good hydride donor. The kinetic intrinsic barrier energy of $iAscH^-$ to release hydride anion in acetonitrile is larger than that of GluNAH to release hydride anion in acetonitrile by 6.9 kcal/mol. The mechanisms of hydride transfer from $iAscH^-$ and GluNAH to phenylxanthium perchlorate ($PhXn^+$), a well-known hydride acceptor, were examined, and the results show that hydride transfer from GluNAH adopted a one-step mechanism, but the hydride transfer from $iAscH^-$ adopted a two-step mechanism ($e-H^\bullet$). The thermodynamic relation charts (TRC) of the $iAscH^-$ family (including $iAscH^-$, $iAscH^\bullet$, $iAsc^{\bullet-}$, and iAsc) and of the GluNAH family (including GluNAH, $GluNAH^{\bullet+}$, $GluNA^\bullet$, and $GluNA^+$) in acetonitrile were constructed as Molecule ID Cards of $iAscH^-$ and of GluNAH in acetonitrile. By using the Molecule ID Cards of $iAscH^-$ and GluNAH, the character chemical properties not only of $iAscH^-$ and GluNAH but also of the various reaction intermediates of $iAscH^-$ and GluNAH all have been quantitatively diagnosed and compared. It is clear that these comparisons of the thermodynamics, kinetics, and mechanisms between $iAscH^-$ and GluNAH as hydride and electron donors in acetonitrile should be quite important and valuable to diagnose and understand the different roles and functions of ascorbic acid and NADH as hydride, hydrogen atom, and electron sources in vivo.

INTRODUCTION

Ascorbic acid ($AscH_2$) ($AscH^-$ exists as the predominant form of $AscH_2$ in physiological pH) and dihydronicotinamide adenine dinucleotide (NADH) are two extremely important natural redox cofactors (Scheme 1), which exist extensively in vivo as effective one-electron (including hydrogen atom) and/or two-electron (including hydride ion) donors to take part in a wide range of biochemical processes.[1,2] For example, as a one-electron donor, ascorbate ($AscH^-$) can reduce dopamine-β-hydroxylase;[3] as a hydrogen atom (or proton-coupled electron) donor, $AscH^-$ can reduce α-tocopheroxyl radical,[4] quinones,[5] peroxynitrite,[6] cytochrome b561,[7] *N*-nitrosated tryptophan,[8] and glutathione peroxidase,[9] etc. In addition, as a two-electron or hydride ion donor, ascorbate ($AscH^-$) can transform into the corresponding dehydroascorbic acid (Asc) in some plants by an ascorbic acid oxidase.[10] Similarly, for NADH, there exist more than 400 enzymatic redox reactions which need NADH to offer electrons or hydride ions in the living body.[11] For example, in the NADH respiratory chain, as a hydride anion (two electrons and a proton) source, NADH can reduce molecular oxygen, flavins, quionones, and cytochrome.[12−15] In the citric acid cycle, as an electron or hydride anion source, NADH can reduce oxaloacetic acid, malic acid, pyruvic acid, oxalosuccinic acid, and α-ketoglutaric acid.[16] Just because ascorbic acid and NADH are two ubiquitous natural organic reducing agents and play very important biochemical roles, the chemistry of ascorbic acid and NADH have drawn extensive interest and high attention of many researchers for a long time.[17−21] Especially, the structures, chemical properties, and biofunctions of the two bioreducing agents in vivo have been the key subjects of extensive studies.[22−25] In order to discover the detailed mechanism of ascorbic acid and NADH as hydride and electron sources, various analogues of ascorbic acid and NADH were designed and synthesized to mimic ascorbic acid and NADH reductions.[26−36] Examining the past publications on the chemistry of ascorbic acid and NADH as hydride and electron sources shows that, although the chemistry, especially the thermodynamics, kinetics, and mechanism of ascorbic acid and NADH reductions have received extensive examination, most attention of chemists all focused on the respective special chemical properties and roles of ascorbic acid and NADH as bioreducing agents,[37−45] no or very little attention has be focused on the differences between ascorbic acid and NADH as hydride and electron sources in thermodynamics,

Received: July 16, 2011
Revised: October 17, 2011
Published: October 30, 2011

dx.doi.org/10.1021/jp2067974 | *J. Phys. Chem. B* 2011, 115, 14794–14811

Scheme 1. Structures of Ascorbic Acid and NADH as Well as Their Corresponding Core Structures

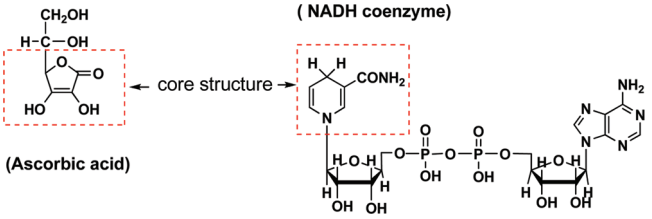

kinetics, and mechanism. In fact, it is quite difficult until now to safely answer the following questions: (1) What are the differences between ascorbic acid and NADH as hydride and electron sources in thermodynamics, kinetics, and mechanism? (2) Why must nature create two water-soluble organic hydride donors, ascorbic acid and NADH, to support life in vivo? (3) Why can ascorbic acid be used as an antioxidant, but NADH cannot? (4) Whether or not the roles and functions of ascorbic acid and NADH as hydride and electron sources in vivo can exchange for each other? It is clear that these scientific questions on the chemistry of ascorbic acid and NADH should be not only fundamental but also very interesting and important, which, of course, have attracted our high attention for a long time. Since most biochemical processes with ascorbic acid and NADH as hydride and electron sources in living body all take place in the polar organic regions constructed with enzyme proteins rather than in the pure aqueous solution, the chemical information of ascorbic acid and NADH as hydride and electron sources in the polar organic regions constructed with enzyme proteins should be more important and valuable than that in the pure aqueous solution. In order to derive the characteristic chemical information of ascorbic acid and NADH as hydride and electron sources in the polar organic regions constructed with enzyme proteins and to answer the questions proposed above, in this work, 5,6-isopropylidene ascorbic acid ($iAscH_2$) and β-D-glucopyranosyl-1,4-dihydronicotinamide acetate (GluNAH) were chosen as the artificial models of ascorbic acid and NADH, respectively (Scheme 2). Acetonitrile was chosen as a polar organic solvent to imitate the polar organic regions constructed with enzyme proteins, because the polarity of acetonitrile (ε = 37.5) is quite close to that of peptide bond in proteins (ε = 37.0, 37.8, and 38.3 for $HCONMe_2$, $MeCONMe_2$ and *N,N*-dimethylbenzamide, respectively).[46]

EXPERIMENTAL SECTION

Materials. Solvents and reagents were obtained from commercial sources and used as received unless otherwise noted. DBU (1,8-diazabicyclo[5.4.0]undec-7-ene) was purchased from Alfa, purified under reduced pressure, and stored in an argon-filled glovebox. Tetrabutylammonium hexafluorophosphate ($(n\text{-}Bu)_4NPF_6$, Aldrich) was recrystallized 3 times from CH_2Cl_2/Et_2O and dried in vacuo at 110 °C for 10 h before preparation of a supporting electrolyte solution. 5,6-Isopropylidene ascorbic acid ($iAscH_2$)[47] and GluNAH[48] were prepared according to the previously described procedures, and were identified by NMR, IR, and MS, respectively. The results are listed: for $iAscH_2$, ^{1}H NMR (400 MHz, DMSO): δ 1.23 (s, 6H), 3.85 (m, 1H), 4.07 (m, 1H), 4.24 (m, 1H), 4.68 (d, 1H), 8.47 (s, 1H), 11.28 (s, 1H); ^{13}C NMR (400 MHz, DMSO): δ 25.7, 64.8, 73.4, 74.1, 108.9, 118.1, 152.2, 161.8, 170.1; IR (KBr): 3042, 3076, 2993, 2906, 2742, 1755, 1662, 1433 cm^{-1}; ESI-MS/M^+ = 216.06. For GluNAH, ^{1}H NMR (400 MHz, $CDCl_3$): δ 2.02−2.06 (m, 12H), 3.10 (s, 2H), 3.76 (m, 1H), 4.12 (m, 1H), 4.25 (m, 1H), 4.39 (d, 1H), 4.88 (m, 1H), 5.10 (m, 1H), 5.23 (m, 2H), 5.40 (s, 1H), 5.99 (d, 1H), 7.11 (s, 1H); ^{13}C NMR (400 MHz, $CDCl_3$): δ 20.5, 20.6, 20.7, 20.8 22.8, 61.9, 68.0, 68.5, 73.1, 74.1, 89.6, 102.1, 104.3, 124.6, 137.5, 169.2, 169.4, 169.6, 180.1,170.7; IR (KBr): 3437, 3342, 3219, 1743, 1689, 1581, 1373 cm^{-1}; ESI-MS/M^+ = 454.10.

Scheme 2. Structures of $iAscH_2$ and GluNAH to Mimic the Core Structures of Ascorbic Acid and NADH Together with Structure of $(G)PhXn^+$ as a Hydride Acceptor

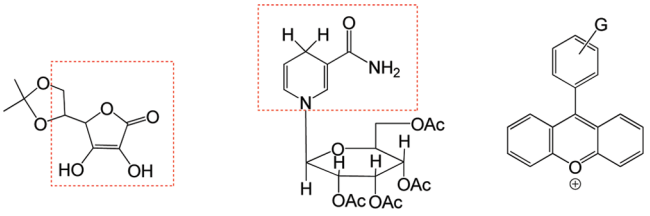

The acetonitrile solutions of 5,6-isopropylidene ascrobate ($iAscH^-$) were obtained by addition of 1 equiv of DBU to solution of 5,6-isopropylidene ascorbic acid ($iAscH_2$) under an inert atmosphere,[26c] and it was characterized by its UV−vis spectroscopy and ^{1}H NMR. Substituted 9-phenylxanthylium perchlorate [$(G)PhXn^+ClO_4^-$] was synthesized according to literature methods.[49] Reagent grade acetonitrile was refluxed over $KMnO_4$ and K_2CO_3 for several hours and was distilled over P_2O_5 under argon twice before use. ^{1}H NMR spectra were recorded in $CDCl_3$ and DMSO-d_6 on Bruker 400 or 300 MHz NMR spectrometer. Chemical shifts are reported in ppm relative to TMS by referencing to residual solvent.

Electrochemistry. The electrochemical experiments were carried out by cyclic voltammetry (CV) and Osteryoung square wave voltammetry (OSWV) using a BAS-100B electrochemical apparatus in deaerated acetonitrile under argon atmosphere. The electrodes used were as follows: working electrode, glassy carbon; reference electrode, 0.01 M $Ag/AgNO_3$ in $(n\text{-}Bu)_4NPF_6/CH_3CN$ electrolyte solution; and auxiliary electrode, platinum wire. Ferrocene/ferrocenium redox couple (Fc/Fc^+) was used as an internal reference for all measurements. Scans were taken at 100 mV s^{-1}. The concentration of the substrate is approximately 1 mM with 0.1 M $(n\text{-}Bu)_4NPF_6$ in acetonitrile. The estimated errors are small than 5 mV.

Isothermal Titration Calorimetry (ITC). The titration experiments were performed on a CSC4200 isothermal titration calorimeter in acetonitrile at 298 K. The performance of the calorimeter was checked by measuring the standard heat of neutralization of an aqueous solution of sodium hydroxide with a standard aqueous HCl solution. Data points were collected every 2 s. The heat of reaction was determined following 10 automatic injections from a 250 μL injection syringe containing a standard solution (~3 mM) into the reaction cell (1.30 mL) containing 1 mL of other concentrated reactant (~10 mM). Injection volume (10 μL) was delivered in a 0.5 s time interval with 300 s between every two injections. The reaction heat was obtained by integration of each peak except the first.[65]

Kinetic Measurements. Kinetic runs were performed on an Applied Photophysics SX.18MV-R stopped-flow spectrophotometer. The SX.18MV-R uses a novel cell cartridge system that has a dead time of around 1 ms with very high sensitivity. All solutions used for kinetics were prepared in an Ar-filled glovebox.

dx.doi.org/10.1021/jp2067974 |J. Phys. Chem. B 2011, 115, 14794–14811

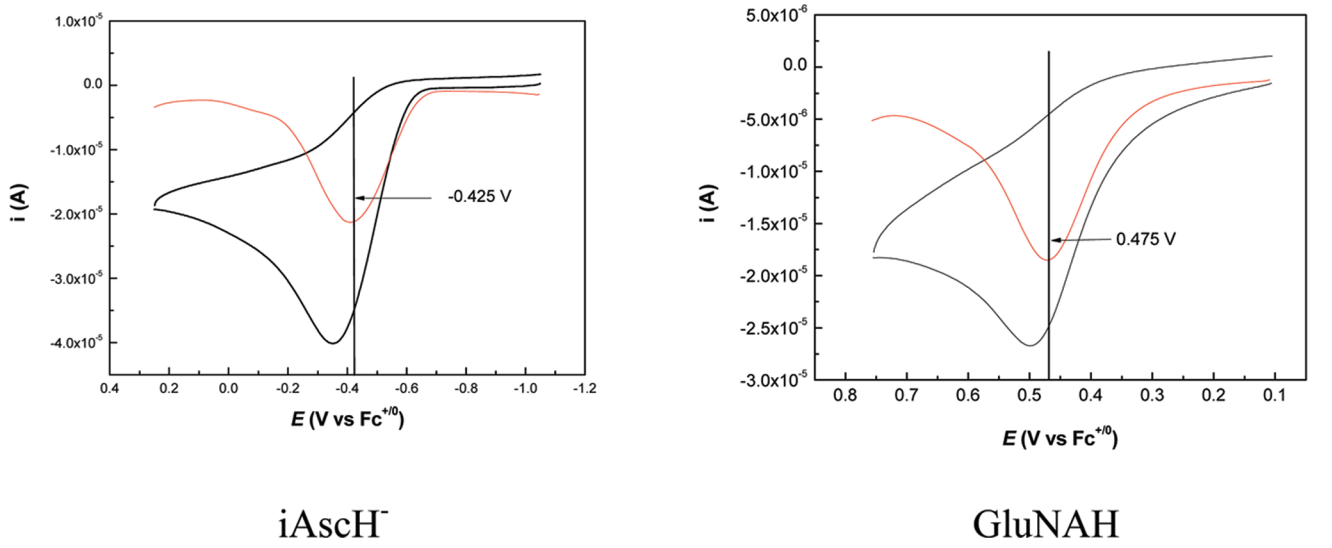

Figure 1. Cyclic voltammogram (CV) and Osteryong square wave voltammogram (OSWV) of $iAscH^-$ and GluNAH in anhydrous deaerated acetonitrile solution containing 0.1 M $(n\text{-}Bu)_4NPF_6$ as supporting electrolyte: CV graph (black line), OSWV graph (red line). The sweep rate is 100 mV/s.

These measurements were under pseudo-first-order conditions for the reactions of GluNAH and $iAscH^-$ with $(G)PhXn^+$, the initial concentrations of GluNAH and $iAscH^-$ ($[GluNAH]_0$ and $[iAscH^-]_0$ for GluNAH and $iAscH^-$, respectively) are more than 20 times over $[(G)PhXn^+]_0$. The pseudo-first-order rate constants were calculated by Guggenheim's method, and then converted to second-order rate constants by linear correlation of the pseudo-first-order rate constants against the concentrations of the excessive reactants. But, for the hydrogen-transfer step in the hydride transfer process from $iAscH^-$ to $(G)PhXn^+$, the second-order rate constants were obtained from slope of the plots of A_t versus $(A_0 - A_t)/t$ by using Origin Software. Eyring activation parameters were derived from Eyring plots. The reaction constant (ρ) of these reactions were obtained according to the equation $\log k = \rho\sigma$, where σ is Hammett substituent parameters.

RESULTS

5,6-Isopropylidene ascorbic acid ($iAscH_2$),[47] GluNAH,[48] and $(G)PhXn^+$ cations[49] were prepared in this work by following the previously described procedure, and identified by ^1H NMR and MS. $iAscH^-$ was generated in situ by addition of 1 equiv of DBU (1,8-diazabicyclo [5.4.0] undec-7-ene) to $iAscH_2$ in CH_3CN according to the literature,[26c] and was characterized by UV−vis spectrophotometry and ^1H NMR spectroscopy. The oxidation potentials of $iAscH^-$, GluNAH, and (G)PhXnH (Figures 1 and 4) as well as the reduction potentials of $GluNA^+$ and $(G)PhXn^+$ in acetonitrile were measured by using CV and OSWV, respectively (Figures 2 and 5). The reduction potential of iAsc in acetonitrile was obtained from the second oxidation peak of $iAsc^{2-}$ in acetonitrile (Figure 3), because the first oxidation peak of $iAsc^{2-}$ is reversible. The detailed results are summarized in Table 1. When $iAscH^-$ and GluNAH were treated by $(G)PhXn^+$ in acetonitrile at room temperature, respectively, the final products are iAsc or $GluNA^+$ and (G)PhXnH and the stoichiometric relationships for the two reactions are all 1 mol per 1 mol, which means that the two reactions (eqs 1 and 2) were completed by hydride transfers. The molar enthalpy change (ΔH_{rxn}) of the

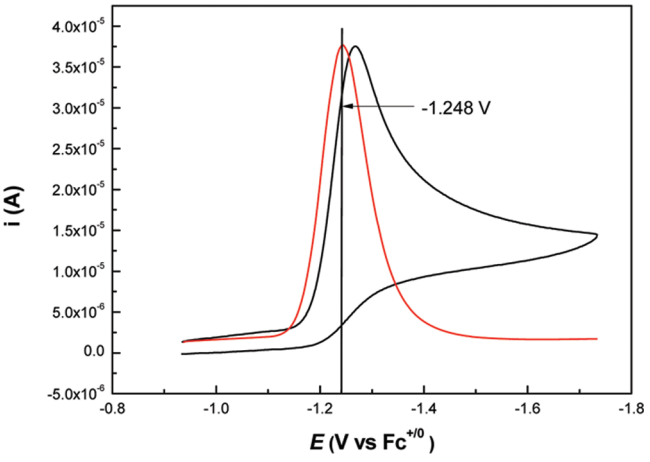

Figure 2. Cyclic voltammogram (CV) and Osteryong square wave voltammogram (OSWV) of $GluNA^+$ in anhydrous deaerated acetonitrile solution containing 0.1 M $(n\text{-}Bu)_4NPF_6$ as supporting electrolyte: CV graph (full line), OSWV graph (red line). The sweep rate is 100 mV/s.

hydride transfer from $iAscH^-$ and GluNAH to $(G)PhXn^+$ in acetonitrile at 298 K was determined by titration calorimetry on a CSC 4200 isothermal titration calorimeter (Figure 6). The detailed results are also listed in Table 1.

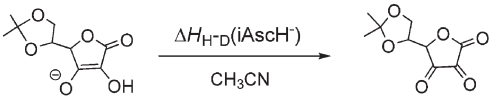

(1)

$$\Delta H_{H\text{-}D}(iAscH^-) = H_f(iAsc) + H_f(H^-) - H_f(iAscH^-) \quad (2)$$

The reduction rates of $(G)PhXn^+$ by $iAscH^-$ and GluNAH in acetonitrile were determined according to monitoring the spectra change of $(G)PhXn^+$ at 449 nm by using an Applied Photophysics SX.18MV-R stopped-flow spectrometer (Figure 7). The second-order rate constants (k_2) for the reactions at different

dx.doi.org/10.1021/jp2067974 |J. Phys. Chem. B 2011, 115, 14794–14811

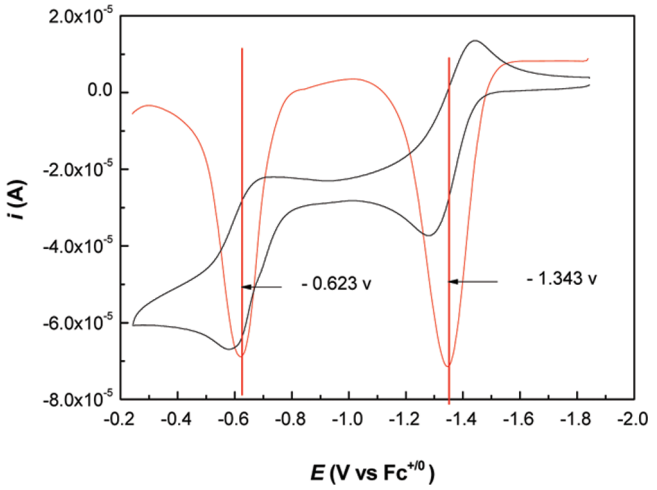

Figure 3. Cyclic voltammogram (CV) and Osteryong square wave voltammogram (OSWV) of $iAsc^{2-}$ in anhydrous deaerated acetonitrile solution containing 0.1 M $(n\text{-}Bu)_4NPF_6$ as supporting electrolyte: CV graph (black line), OSWV graph (red line). The sweep rate is 100 mV/s.

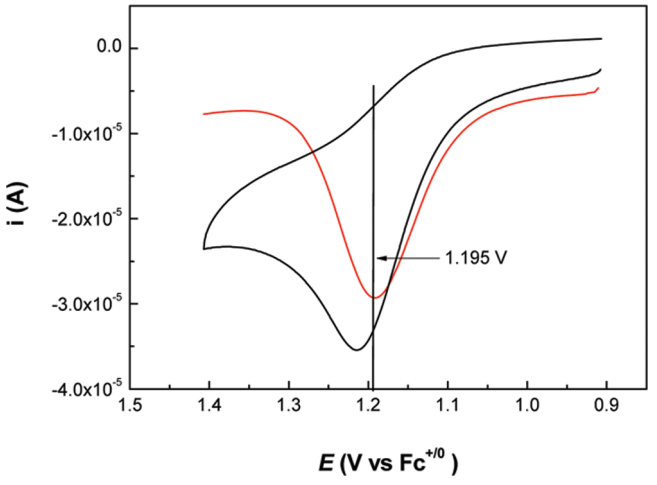

Figure 4. Cyclic voltammogram (CV) and Osteryong square wave voltammogram (OSWV) of PhXnH in anhydrous deaerated acetonitrile solution containing 0.1 M $(n\text{-}Bu)_4NPF_6$ as supporting electrolyte: CV graph (black line), OSWV graph (red line). The sweep rate is 100 mV/s.

temperatures between 288 and 308 K are listed in Tables 2 and 4, respectively. Activation parameters activation enthalpy ($\Delta H^{\ddagger}$) and activation entropy ($\Delta S^{\ddagger}$) of the two reactions were derived from the slope and intercept of the Eyring plots of $\ln(k_2/T)$ versus the reciprocal of the absolute temperature ($1/T$), which are listed in Tables 3 and 4, respectively. Due to formation of a new reaction intermediate (λ_{max} = 372 nm) during the hydride transfer from $iAscH^-$ to $(G)PhXn^+$ in acetonitrile, the formation and decay kinetics of the reaction intermediate in the reaction was also examined according to the UV−vis absorption change of the reaction intermediate. The experimental results showed that the formation rate of the reaction intermediate was equal to the decay rate of $(G)PhXn^+$ (Figure 8), indicating that the formation of the reaction intermediate was directly derived from the transformation of $iAscH^-$ or $(G)PhXn^+$ by electron or hydrogen atom transfer. But the decay rate of the reaction intermediate is much slower than the formation rate and obeys

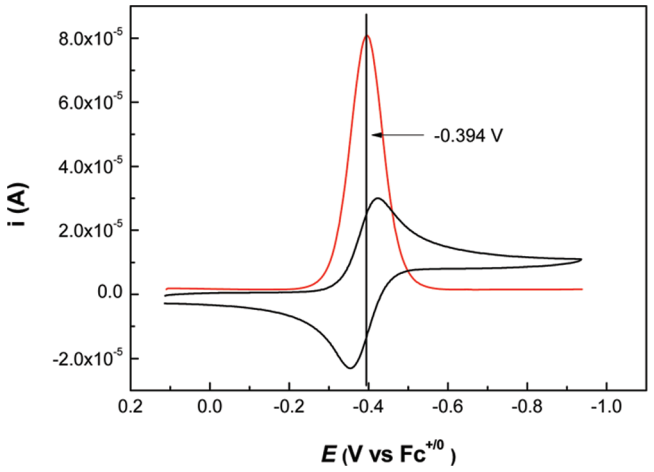

Figure 5. Cyclic voltammogram (CV) and Osteryong square wave voltammogram (OSWV) of $PhXn^+$ in anhydrous deaerated acetonitrile solution containing 0.1 M $(n\text{-}Bu)_4NPF_6$ as supporting electrolyte: CV graph (black line), OSWV graph (red line). The sweep rate is 100 mv/s.

Table 1. Oxidation Potentials of $iAscH^-$, GluNAH, and $(G)PhXnH$, Reduction Potentials of iAsc, $GluNA^+$ and $(G)PhXn^+$ as Well as Reaction Enthalpy Changes of $iAscH^-$ and GluNAH with $(G)PhXn^+$ in Dry Acetonitrile

	$E_{ox}(XH)^a$		$E_{red}(X^+)^a$		$\Delta H_{rxn}{}^b$	
X^+	CV	OSWV	CV	OSWV	$iAscH^-$	GluNAH
iAsc	−0.380	−0.425	−0.595	−0.623		
$GluNA^+$	0.503	0.475	−1.269	−1.248		
$(G)PhXn^+$						
p-CF_3	1.287	1.257	−0.335	−0.336	−18.1	−24.1
m-CF_3	1.274	1.241	−0.343	−0.343	−17.7	−23.7
p-Cl	1.257	1.220	−0.353	−0.355	−17.3	−23.3
p-Br	1.249	1.208	−0.361	−0.360	−17.0	−23.0
m-OCH_3	1.235	1.201	−0.374	−0.373	−16.7	−22.7
p-H	1.227	1.195	−0.394	−0.394	−16.2	−22.2
m-CH_3	1.215	1.188	−0.409	−0.408	−15.8	−21.8
p-CH_3	1.206	1.176	−0.412	−0.413	−15.4	−21.4
p-OCH_3	1.190	1.160	−0.430	−0.430	−14.9	−20.9

[a] Measured by CV and OSWV methods in dry acetonitrile at room temperature, the unit in volts vs $Fc^{+/0}$ and reproducible to 5 mV or better. [b] ΔH_{rxn} was obtained from the reaction heats of eqs 1 and 2 by switching the sign; the latter were measured by titration calorimetry in dry acetonitrile at 298 K. The data, given in kcal/mol, were average values of at least three independent runs. The reproducibility is ±0.5 kcal/mol.

the second-order rather than the first-order kinetic law, meaning that decay of the reaction intermediate was due to the reaction of the two separated rather than bonded reaction partners. If the initial concentration of the excess reactant ($iAscH^-$) was changed, the decay rate of the reaction intermediate has no change, which means that the decay of the reaction intermediate is not dependent on the remained initial reactant. The second-order rate constants (k_2) of the reaction intermediate decay at different temperatures between 288 and 308 K and the activation parameters: activation enthalpy ($\Delta H^{\ddagger}$), activation entropy ($\Delta S^{\ddagger}$), and

dx.doi.org/10.1021/jp2067974 |J. Phys. Chem. B 2011, 115, 14794–14811

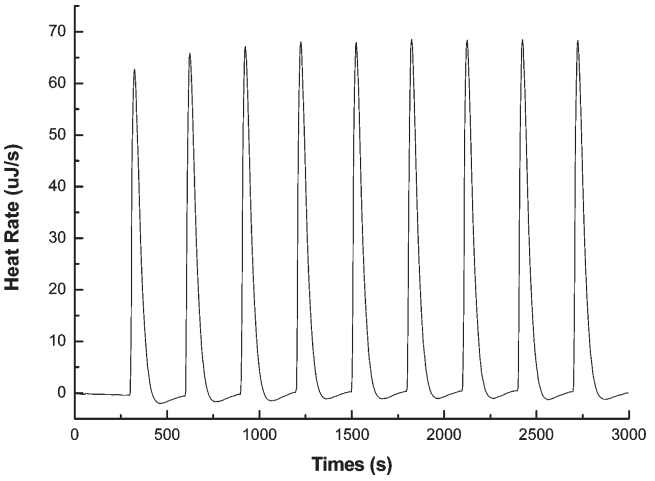

Figure 6. Isothermal titration calorimetry (ITC) for the reaction heat of $iAscH^-$ with 9-phenylxanthium perchlorate ($9\text{-}PhXn^+ClO_4^-$) in acetonitrile at 298 K. Titration was conducted by adding 10 μL of $9\text{-}PhXn^+ClO_4^-$ (5.26 mM) every 300s into the acetonitrile containing $iAscH^-$ (ca. 20 mM).

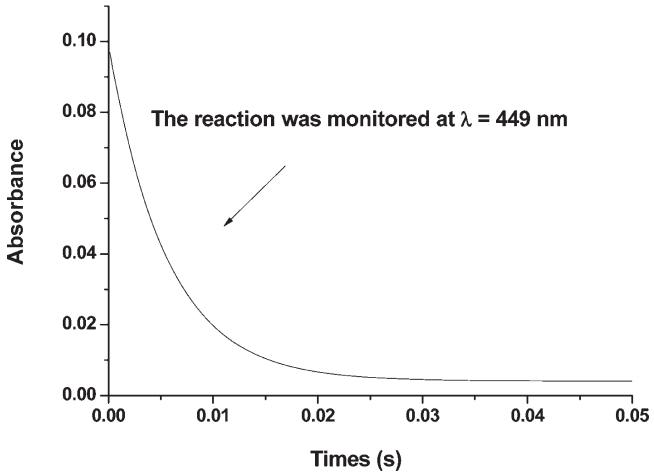

Figure 7. Time-resolved spectrum at 449 nm due to $PhXn^+$ for the reaction of $iAscH^-$ (1×10^{-2} M) with $PhXn^+$ (4×10^{-4} M) in dry acetonitrile at 298 K.

activation free energy ($\Delta G^{\ddagger}$) are listed in Tables 2 and 3, respectively.

DISCUSSION

Comparison of Chemical Properties of $iAscH^-$ and GluNAH as Well as Their Various Reaction Intermediates as Hydride, Electron, Hydrogen Atom, and Proton Donors. Since $AscH^-$ and NADH can act not only as a hydride donor but also as a hydrogen atom donor and an electron donor in vivo, and the chemical processes of hydride transfer from $AscH^-$ and NADH often involve multistep mechanism besides the hydride one-step transfer mechanism (Scheme 3), it is conceived that the following chemical processes are all possible to take place in vivo: (1) $AscH^-$ and NADH release a hydride anion, a hydrogen atom and an electron. (2) The intermediates $AscH^•$ and $NADH^{•+}$ release a hydrogen atom and a proton. (3) The intermediates $Asc^{•-}$ and $NAD^•$ release an electron. In order to quantitatively describe and compare the characteristic chemical behaviors of $AscH^-$ and NADH as well as their corresponding various reaction intermediates in vivo, the thermodynamic driving forces of $iAscH^-$ and GluNAH as $AscH^-$ and NADH models to release hydride, hydrogen atom, and electron, the thermodynamic driving forces of $iAscH^•$ and $GluNAH^{•+}$ as $AscH^•$ and $NADH^{•+}$ models to release hydrogen atom and proton as well as the thermodynamic driving forces of $iAsc^{•-}$ and $GluNA^•$ as $Asc^{•-}$ and $NAD^•$ models to release electron in acetonitrile all need examination in detail.

In this work, thermodynamic driving forces of $iAscH^-$ and GluNAH as well as $iAsc^{•-}$ and $GluNA^•$ to release electron can be expressed by their oxidation potentials, but the thermodynamic driving forces of $iAscH^-$ and GluNAH as well as their reaction intermediates $iAscH^•$ and $GluNAH^{•+}$ to release hydride, hydrogen atom, and proton were defined as the enthalpy changes of the corresponding chemical processes.[50] The enthalpy changes of $iAscH^-$ and GluNAH to release hydride anion in acetonitrile can be obtained from the reaction enthalpy change (ΔH_{rxn}) of hydride transfer from $iAscH^-$ and GluNAH to 9-phenylxanthium perchlorate ($PhXn^+ClO_4^-$) in acetonitrile (eqs 3 and 4). In eq 4, ΔH_{rxn} were measured by using titration calorimetry in acetonitrile (Figure 6), and $\Delta H_{H^-A}(PhXn^+)$ is the hydride affinity of $PhXn^+$ in acetonitrile, which can be available from our previous work (−96.8 kcal/mol).[51] The thermodynamic driving forces of $iAscH^-$ and GluNAH to release hydrogen atom in acetonitrile and the thermodynamic driving forces of $iAscH^•$ and $GluNAH^{•+}$ to release hydrogen atom and proton can be derived from eqs 5−7,[52] respectively. The three eqs 5−7 can be derived from the three thermodynamic cycles according to Hess's law,[53,54] respectively. The results are all summarized in Table 5. In order to conveniently compare the chemical properties of $iAscH^-$ and GluNAH as well as their various corresponding reaction intermediates, the thermodynamic relation charts of $iAscH^-$ family (including $iAscH^-$, $iAscH^•$, $iAsc^{•-}$, and iAsc) and GluNAH family (including GluNAH, $GluNAH^{•+}$, $GluNA^•$, and $GluNA^+$) (Scheme 5) were constructed using the determined six thermodynamic parameters listed in Table 5, which can be defined as Molecule ID Cards of $iAscH^-$ and GluNAH.[52] From the Molecule ID Cards of $iAscH^-$ and GluNAH, three different character thermodynamic parameters can be obtained for each member in the $iAscH^-$ family and GluNAH family, which can be used to quantitatively describe the three different characteristic chemical properties of the members in $iAscH^-$ family and GluNAH family at the same time. The results are listed in Tables 6 and 7, respectively.

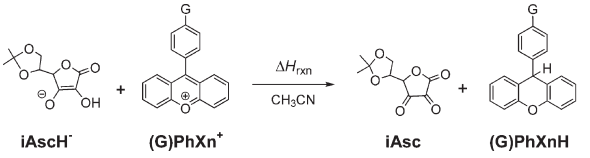

(3)

$$\Delta H_{H\text{-}D}(iAscH^-) = \Delta H_{rxn}(\text{eq } 3) - H_{H\text{-}A}(PhXn^+) \quad (4)$$

$$\Delta H_{HD}(iAscH^-) = \Delta H_{H\text{-}D}(iAscH^-) - F[E^o_{red}(iAsc) - E^o(H^{0/-})] \quad (5)$$

$$\Delta H_{PD}(iAscH^•) = \Delta H_{HD}(iAscH^-) - F[E^o_{ox}(iAscH^-) - E^o(H^{+/0})] \quad (6)$$

$$\Delta H_{HD}(iAscH^•) = \Delta H_{H\text{-}D}(iAscH^-) - F[E^o_{ox}(iAscH^-) - E^o(H^{0/-})] \quad (7)$$

Table 2. Dependence of the Reaction Rates of the First Step and the Second Step Hydride Transfer from iAscH$^-$ to (G)PhXn$^+$ in Acetonitrile on the Reaction Temperature

	k_2 for the first step ($\times 10^{-4}$ M^{-1} s^{-1}) [a]				
(G)PhXn$^+$	288 K	293 K	298 K	303 K	308 K
p-CF_3	5.71	7.84	9.37	12.03	13.84
m-CF_3	5.10	7.09	8.49	10.48	12.41
p-Cl	4.15	6.04	7.21	9.29	10.41
p-Br	4.02	5.56	6.29	8.85	9.88
m-OCH_3	3.69	5.15	6.43	7.70	9.12
p-H	3.45	4.38	5.50	7.13	8.14
m-CH_3	3.19	4.24	5.22	6.78	7.66
p-CH_3	2.88	3.90	4.73	5.73	7.19
p-OCH_3	2.42	3.36	4.29	5.23	6.02
	k_2 for the second step ($\times 10^{-1}$ M^{-1} s^{-1}) [b]				
(G)PhXn$^+$	288 K	293 K	298 K	303 K	308 K
p-CF_3	7.22	8.31	10.02	11.59	13.00
m-CF_3	7.03	7.90	9.57	11.18	12.80
p-Cl	6.79	7.57	9.34	10.79	12.35
p-Br	6.55	7.29	9.14	10.60	12.03
m-OCH_3	6.32	7.16	9.00	10.39	11.84
p-H	6.08	7.10	8.75	10.28	11.64
m-CH_3	5.80	6.78	8.50	9.99	11.50
p-CH_3	5.59	6.53	8.39	9.60	11.29
p-OCH_3	5.38	6.29	8.10	9.29	10.98

[a] Second-order rate constants k_2 for the first step of the hydride transfer from iAscH$^-$ to (G)PhXn$^+$ were obtained from the corresponding pseudo-first-order rate constants by the linear correlation against the concentration of the (G)PhXn$^+$, the experimental error is within 5%. [b] Second-order rate constants k_2 for the second step of the hydride transfer from iAscH$^-$ to (G)PhXn$^+$ were obtained by using second-order kinetic fitting method for the decay lines of the initially formed reaction intermediate iAscH$^\bullet$, the experimental error is within 5%.

Comparison of Reaction Mechanism of iAscH$^-$ and GluNAH as Hydride Sources. Although iAscH$^-$ and GluNAH all can be used as hydride ion donors, the mechanisms of the hydride transfer from the two hydride donors are generally different, because the difference of redox properties between iAscH$^-$ and GluNAH is quite large (ΔE = 0.900 V). In fact, the mechanism of the hydride transfer from NADH and AscH$^-$ to a two-electron acceptor (i.e., a hydride acceptor) is still a disputed question so far.[5,15,32d,56,57] The controversy focus is whether the mechanism of the hydride transfer is a one-step or multistep sequence involving electron transfer as the initial step: electron−proton−electron, electron−hydrogen, or hydrogen−electron. One of the main reasons resulting in the difficulty to elucidate the hydride transfer mechanism is that no detailed energetic data of each possible mechanistic step for the hydride transfer are available. From this work, we not only have obtained the thermodynamic driving forces of iAscH$^-$ and GluNAH as hydride donors to release a hydride anion, to release a hydrogen atom, and to release an electron, as well as the thermodynamic driving forces of the various reaction intermediates of iAscH$^-$ and GluNAH to release a hydrogen atom, to release a proton, and to release an electron, but also have obtained the thermodynamic driving forces of (G)PhXn$^+$ as hydride acceptors to obtain a hydride anion, to obtain a hydrogen atom, and to obtain an electron, as well as the thermodynamic driving forces of the various reaction intermediates of (G)PhXn$^+$ to obtain a hydrogen atom, to obtain a proton, and to obtain an electron. These thermodynamic data may been used to construct the Molecule ID Card of iAscH$^-$ or GluNAH and (G)PhXn$^+$.[58] It is easy to examine the thermodynamics of the detailed mechanistic steps of the hydride transfer from iAscH$^-$ and GluNAH to (G)PhXn$^+$ according to the thermodynamic analytic platforms which consist of the Molecule ID Cards of iAscH$^-$ or GluNAH and (G)PhXn$^+$ (Schemes 6 and 7). The detailed results of the standard-state free energy change of each elementary step for

Table 3. Activation Parameters for the First Step and Second Step of the Hydride Transfer from iAscH$^-$ to (G)PhXn$^+$ in Dry Acetonitrile

	for the first step				for the second step			
(G)PhXn$^+$	$\Delta H^{\ddagger a}$	$\Delta S^{\ddagger b}$	$-T\Delta S^{\ddagger c}$	$\Delta G^{\ddagger d}$	$\Delta H^{\ddagger a}$	$\Delta S^{\ddagger b}$	$-T\Delta S^{\ddagger c}$	$\Delta G^{\ddagger d}$
p-CF_3	7.17	−11.72	3.50	10.67	4.88	−33.04	9.85	14.73
m-CF_3	7.07	−12.28	3.66	10.73	5.01	−32.67	9.74	14.75
p-Cl	7.44	−11.37	3.39	10.83	5.03	−32.68	9.74	14.77
p-Br	7.40	−11.64	3.47	10.87	5.18	−32.23	9.60	14.78
m-OCH_3	7.24	−12.33	3.67	10.91	5.31	−31.81	9.48	14.80
p-H	7.18	−12.76	3.80	10.98	5.46	−31.36	9.34	14.81
m-CH_3	7.27	−12.58	3.75	11.02	5.78	−30.36	9.05	14.83
p-CH_3	7.22	−12.92	3.85	11.08	5.90	−30.01	8.94	14.85
p-OCH_3	7.43	−12.56	3.73	11.16	6.00	−29.73	8.86	14.87

[a] From the slopes of the Eyring plots, the unit is kcal mol^{-1}, and the uncertainty is smaller than 0.05 kcal/mol. [b] From the intercepts of the Eyring plots, the unit is cal mol^{-1} K^{-1}, the uncertainty is smaller than 0.04 cal mol^{-1} K^{-1}. [c] The unit is kcal mol^{-1}. [d] From the equation $\Delta G^{\ddagger} = \Delta H^{\ddagger} - T\Delta S^{\ddagger}$, the unit is kcal mol^{-1}.

Table 4. Dependence of k_2 for the Hydride Transfer from GluNAH to (G)PhXn$^+$ in Acetonitrile on the Reaction Temperature Together with the Corresponding Activation Parameters

	$k_2 \times 10^{-4a}$								
(G)PhXn$^+$	288 K	293 K	298 K	303 K	308 K	$\Delta H^{\ddagger b}$	$\Delta S^{\ddagger c}$	$-T\Delta S^{\ddagger d}$	$\Delta G^{\ddagger e}$
p-CF_3	10.51	10.99	11.38	11.72	12.02	0.53	34.16	10.01	10.54
m-CF_3	9.10	9.39	9.78	10.02	10.42	0.54	34.47	10.10	10.64
p-Cl	5.97	6.28	6.62	6.86	7.06	0.85	34.23	10.03	10.88
p-Br	5.75	5.98	6.15	6.33	6.61	0.54	35.39	10.37	10.91
m-OCH_3	4.44	4.65	4.94	5.40	5.66	1.54	32.42	9.50	11.04
p-H	3.22	3.45	3.78	3.95	4.16	1.60	32.80	9.61	11.22
m-CH_3	2.56	2.87	3.06	3.26	3.45	1.87	32.29	9.46	11.33
p-CH_3	1.78	1.95	2.14	2.31	2.45	2.14	32.12	9.41	11.55
p-OCH_3	1.41	1.57	1.67	1.81	1.95	2.10	32.76	9.60	11.70

[a] Second-order rate constants k_2 for the hydride transfer from GluNAH to (G)PhXn$^+$ in acetonitrile were obtained from the corresponding pseudo-first-order rate constants by the linear correlation against the concentration of the (G)PhXn$^+$, the experimental error is within 5%. [b] From the slop of the Eyring plots, the unit is kcal mol^{-1}, and the uncertainty is smaller than 0.05 kcal mol^{-1}. [c] From the intercept of the Eyring plots, the unit is cal mol^{-1} K^{-1}, and the uncertainty is smaller than 0.04 cal mol^{-1} K^{-1}. [d] The unit is kcal mol^{-1}. [e] From the equation $\Delta G^{\ddagger} = \Delta H^{\ddagger} - T\Delta S^{\ddagger}$, the unit is kcal mol^{-1}.

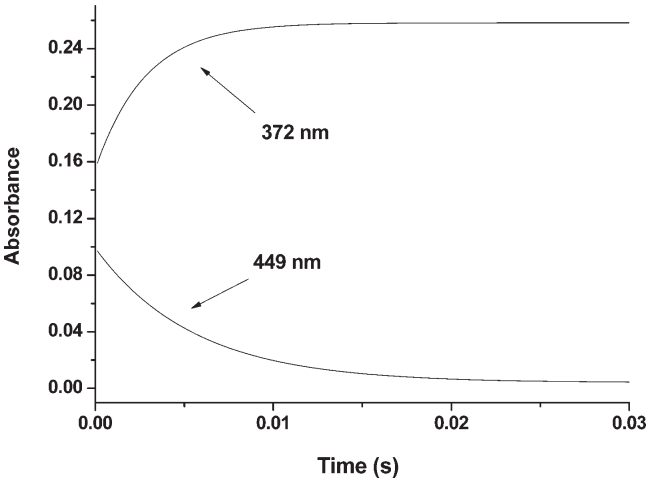

Figure 8. UV−vis spectrum plots of $PhXn^+$ at λ = 449 nm and a reaction intermediate at λ = 372 nm against the reaction time. The initial reaction condition: the concentration of $iAscH^-$ and $PhXn^+$ is 1×10^{-2} and 4×10^{-4} M, respectively, in dry acetonitrile at 298 K.

the hydride transfer from $iAscH^-$ and GluNAH to $(G)PhXn^+$ are summarized in Table 8.

From Scheme 6 and Table 8 it is easy to find that for the hydride transfer from GluNAH to $(G)PhXn^+$, the state energy change scales of the three initial steps (steps *a*, *b*, and *c*) in the four possible pathways range from 18.7 to 20.9 kcal/mol for the electron transfer (step *a*), from 33.6 to 34.8 kcal/mol for the hydrogen transfer (step *b*), and from −24.1 to −20.9 kcal/mol for the concerted hydride transfer (step *c*). Since the state energy changes for the concerted hydride transfer (step *c*) are all quite negative (more negative than −20.9 kcal mol^{-1}), and the state energy changes for the electron transfer and for hydrogen transfer are all quite positive (more positive than 18.7 kcal mol^{-1}), it is reasonable to suggest that the electron-transfer process (step *a*) and the hydrogen-transfer process (step *b*) all can be ruled out as the initial step for the reaction of GluNAH with $(G)PhXn^+$; as a result, the remaining concerted hydride transfer step (step *c*) should be merely the reasonable pathway for the reaction of GluNAH with $(G)PhXn^+$ in acetonitrile.

In order to further verify the reaction mechanism of GluNAH with $(G)PhXn^+$ in acetonitrile, the kinetics of hydride transfer from GluNAH to $(G)PhXn^+$ in acetonitrile was examined. From Table 4, it is found that activation free energetic scales of the hydride transfer from GluNAH to $(G)PhXn^+$ range from 10.5 to 11.7 kcal mol^{-1}, which are much smaller than the standard-state energy changes of the initial electron transfer (step *a*) (18.7−20.9 kcal/mol), and also much smaller than the standard-state energy changes of the initial hydrogen-transfer (step *b*) (33.6−34.8 kcal/mol), but larger than the standard-state energy change of the concerted hydride transfer (step *c*) (−24.1 to −20.9 kcal/mol). According to the transition-state theory that the activation free energy change is always larger than or at least equal to the corresponding standard-state free energy change for any elemental reaction,[59] it is evident that both of the reaction steps *a* and *b* should be ruled out as the initial reaction in the reactions of GluNAH with $(G)PhXn^+$, and the only remaining step *c* is suitable for the reaction law (Figure 10).

By comparing $\Delta H^{\ddagger}$ and $-T\Delta S^{\ddagger}$ of the hydride transfer from GluNAH to $(G)PhXn^+$ in Table 4, it is found that the values of $\Delta H^{\ddagger}$ are generally much smaller than those of the corresponding $-T\Delta S^{\ddagger}$, which means that the main activation energy block for the hydride transfer from GluNAH to $(G)PhXn^+$ is entropy change rather than enthalpy change. This comparison also supports that the hydride transfer from GluNAH to $(G)PhXn^+$ in acetonitrile really took the concerted one step.

Scheme 3. Possible Pathways of the Hydride Transfer from $iAscH^-$

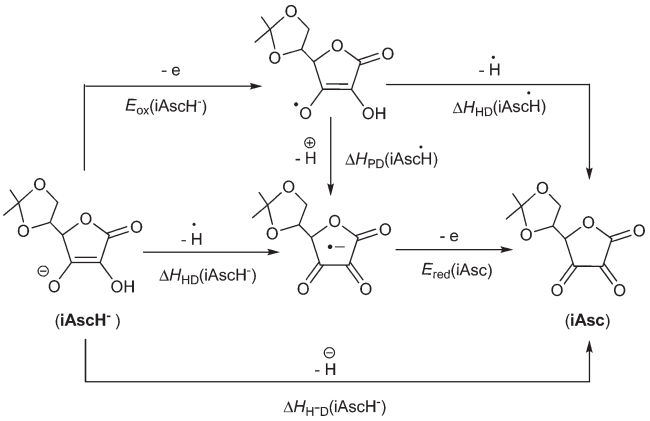

From Scheme 7 and Table 8, it is also easy to find that for the hydride transfer from $iAscH^-$ to $(G)PhXn^+$, the state energy change scales of the three initial steps (steps *a*, *b*, and *c*) in the four possible pathways (Scheme 7) range from −2.1 to 0.1 kcal for the electron transfer (step *a*), from 25.2 to 26.4 kcal/mol for the hydrogen transfer (step *b*), and from −18.1 to −14.9 kcal/mol for the concerted hydride transfer (step *c*). Since the state energy changes for the hydrogen-transfer (step *b*) all are quite positive (more positive than 25.2 kcal/mol), it is reasonable to suggest that the hydrogen atom transfer process may be ruled out as the initial step for the hydride transfer. For step *c*, since the state energy changes all are quite negative (more negative than −14.9 kcal/mol), it is evident that the concerted hydride transfer mechanism (step *c*) should be most likely. As to the initial electron transfer (step *a*), the possibility of the initial electron transfer cannot be ruled out, because the thermodynamic block for the electron transfer is none or too small (−2.1 to 0.1 kcal/mol). In addition, the intrinsic barrier energies of electron transfers are generally much smaller than that of hydride transfers,[60] which would also favor the electron transfer. It is evident that from the view of thermodynamics there exist at least three possible mechanisms for the hydride transfer from $iAscH^-$ to $(G)PhXn^+$ in acetonitrile: the concerted hydride one-step transfer (step *c*), the hydrogen transfer initiated by electron transfer (steps *a* and *d*, i.e., e−$H^{\bullet}$), and the initial electron transfer followed by proton and electron transfer separately (steps *a*, *e*, and *f*, i.e., e−p−e). However, the mechanism of e−p−e three steps may be ruled out, because the thermodynamic block for the proton transfer from $iAscH^{\bullet}$ to $(G)PhXn^{\bullet}$ in acetonitrile (step *e*) is too high (26.2−27.3 kcal/mol).

In order to further diagnose the real reaction mechanism of hydride transfer from $iAscH^-$ to $(G)PhXn^+$, the intermediate products of the hydride transfer from $iAscH^-$ to $(G)PhXn^+$ in dry acetonitrile were detected. The results are shown in Figures 8 and 9. From Figure 8, it is clear that when $PhXn^+$ (4×10^{-4} M) was mixed with excess $iAscH^-$ (1×10^{-2} M) in acetonitrile, the UV−vis absorbance of $PhXn^+$ (449 nm) was rapidly decreased with the reaction time, and meanwhile a new absorbance at 372 nm

Table 5. Molar Enthalpy Changes of $iAscH^-$ and GluNAH as Well as (G)PhXnH (XH) To Release Hydride Anions and Hydrogen Atoms, and the Molar Enthalpy Changes of $XH^{\bullet+}$ To Release Hydrogen Atoms and Protons (kcal mol^{-1}) as Well as Oxidation Potentials of XH and $X^\bullet$ in Acetonitrile (V versus $Fc^{+/0}$)

XH	$\Delta H_{H^-D}(XH)^a$	$\Delta H_{HD}(XH)^b$	$E_{ox}(XH)^c$	$\Delta H_{PD}(XH^{\bullet+})^b$	$\Delta H_{HD}(XH^{\bullet+})^b$	$E_{ox}(X^\bullet)^c$
$iAscH^-$	80.6	69.0	−0.425	25.8	64.4	−0.623
GluNAH	74.6	77.4	0.475	13.5	37.6	−1.248
(G)PhXnH						
p-CF_3	98.7	80.4	1.257	−1.5	43.7	−0.336
m-CF_3	98.3	80.2	1.241	−1.4	43.7	−0.343
p-Cl	97.9	80.1	1.220	−1.1	43.8	−0.355
p-Br	97.6	79.9	1.208	−1.0	43.7	−0.360
m-OCH_3	97.3	79.9	1.201	−0.6	43.6	−0.381
p-H	96.8	79.9	1.195	−0.7	43.2	−0.394
m-CH_3	96.4	79.8	1.188	−0.6	43.0	−0.408
p-CH_3	96.0	79.5	1.176	−0.6	42.9	−0.413
p-OCH_3	95.5	79.4	1.164	−0.4	42.6	−0.430

[a] $\Delta H_{H^-D}(XH)$ values for XH = $iAscH^-$ and GluNAH were derived from eq 4, take $\Delta H_{H^-A}(PhXn^+) = -96.8$ kcal/mol in acetonitrile from ref 51; the $\Delta H_{H^-D}(XH)$ values for XH = (G)PhXnH were derived from the corresponding enthalpy change of $(G)PhXn^+$ with $iAscH^-$ in acetonitrile minus $\Delta H_{H^-D}(iAscH^-)$ (80.6 kcal/mol). The uncertainties are all smaller than 1 kcal/mol. [b] $\Delta H_{HD}(XH)$, $\Delta H_{PD}(XH^{\bullet+})$, and $\Delta H_{HD}(XH^{\bullet+})$ were estimated from eqs 5−7, respectively, taking $E^o(H^{0/-}) = -1.128$ V vs Fc and $E^o(H^{+/0}) = -2.298$ V vs Fc in acetonitrile from Zhang's work.[55] The relative uncertainties were estimated to be smaller than or close to 1 kcal/mol in each case. [c] The standard oxidation potentials of XH and $X^\bullet$ in acetonitrile were derived from the experimental results by using CV method, but if the electrochemical oxidations of XH or $X^\bullet$ are irreversible, the standard oxidation potentials of XH and $X^\bullet$ in acetonitrile were derived from the OSWV results, because OSWV has been verified to be more exact electrochemical method for evaluating the standard one-electron redox potentials of analyte with irreversible electrochemical processes than CV.[50]

Scheme 4. Three Thermodynamic Cycles Constructed on the Basis of the Chemical Process of $iAscH^-$ To Release Hydride Anion in Acetonitrile

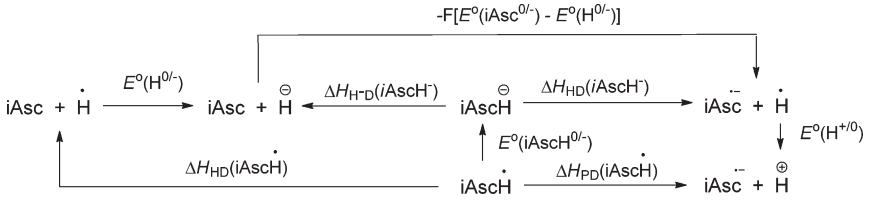

Scheme 5. Molecule ID Cards of $iAscH^-$ and GluNAH in Acetonitrile

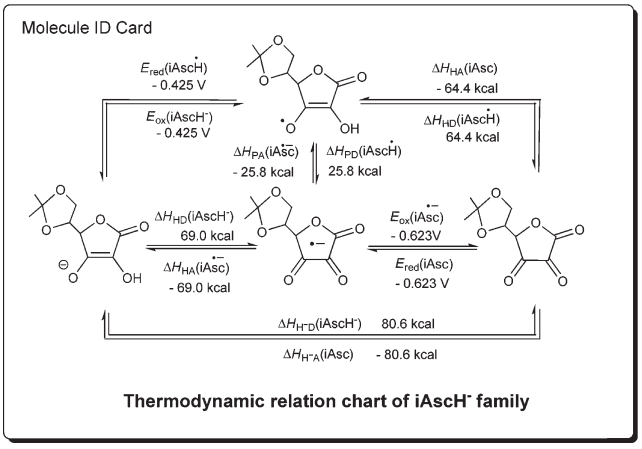

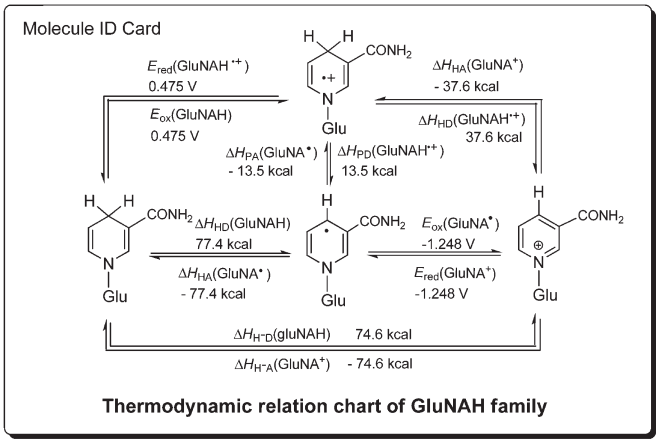

appeared, and the increase of the absorption at 372 nm was synchronous with the decrease of the absorption at 449 nm, which means that the species with absorption at 372 nm was directly derived from $PhXn^\bullet$ or $iAscH^\bullet$. That is, the species with absorption at 372 nm may belong to either $PhXn^\bullet$ or $iAscH^\bullet$. But when the substituted $PhXn^+$, such as $(p\text{-}CH_3O)PhXn^+$, was used to replace

dx.doi.org/10.1021/jp2067974 |J. Phys. Chem. B 2011, 115, 14794–14811

Table 6. Diagnoses of Chemical Properties for the Members in $AscH^-$ Family According to the Molecule ID Card of $iAscH^-$ (Scheme 5)

species	thermodynamic parameters*	diagnoses of the characteristic properties
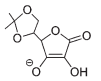	$\Delta H_{H\text{-}D}(iAscH^-) = 80.6$ kcal $\Delta H_{HD}(iAscH^-) = 69.0$ kcal $E_{ox}(iAscH^-) = -0.425$ V	weak hydride donor, weak nucleophilic agent good hydrogen donor and antioxidant strong one-electron reductant
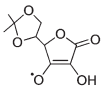	$\Delta H_{PD}(iAscH^{\bullet}) = 25.8$ kcal $\Delta H_{HD}(iAscH^{\bullet}) = 64.4$ kcal $E_{red}(iAscH^{+\bullet}) = -0.425$ V	quite weak organic acid good hydrogen donor and antioxidant poor one-electron oxidant
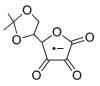	$\Delta H_{PA}(iAsc^{-\bullet}) = -25.8$ kcal $\Delta H_{HA}(iAsc^{-\bullet}) = -69.0$ kcal $E_{ox}(iAsc^{-\bullet}) = -0.623$ V	strong base good hydrogen acceptor, good antioxidant strong one-electron donor
	$\Delta H_{H\text{-}A}(iAsc) = -80.6$ kcal $\Delta H_{HA}(iAsc) = -64.4$ kcal $E_{red}(iAsc) = -0.623$ V	good hydride acceptor and electrophilic agent good hydrogen acceptor, weak antioxidant middle-strong one-electron oxidant

*Note: $\Delta H_{PA}(iAsc^{\bullet-})$, $\Delta H_{HA}(iAsc^{\bullet-})$, $\Delta H_{H\text{-}A}(iAsc)$, and $\Delta H_{HA}(iAsc)$ are defined as the enthalpy changes of $iAsc^{\bullet-}$ to obtain proton and to obtain hydrogen atom, and the enthalpy changes of iAsc to obtain hydride anion and to obtain hydrogen in acetonitrile, respectively. The values are equal to the enthalpy changes of the corresponding opposite species to release proton, to release hydrogen atom, and to release hydride anion in acetonitrile by switching the signs.

Table 7. Diagnoses of Chemical Properties for the Members in GluNAH Family According to the Molecule ID Card of GluNAH (Scheme 5)

species	thermodynamic parameters*	diagnoses of the characteristic properties
	$\Delta H_{H\text{-}D}(GluNAH) = 74.6$ kcal $\Delta H_{HD}(GluNAH) = 77.4$ kcal $E_{ox}(GluNAH) = 0.475$ V	middle-strong hydride donor middle-strong hydrogen donor and antioxidant weak one-electron donor
	$\Delta H_{PD}(GluNAH^{+\bullet}) = 13.5$ kcal $\Delta H_{HD}(GluNAH^{+\bullet}) = 37.6$ kcal $E_{red}(GluNAH^{+\bullet}) = 0.475$ V	strong organic acid strong hydrogen donor and antioxidant strong one-electron oxidant
	$\Delta H_{PA}(GluNA^{\bullet}) = -13.5$ kcal $\Delta H_{HA}(GluNA^{\bullet}) = -77.4$ kcal $E_{ox}(GluNA^{\bullet}) = -1.248$ V	not strong base middle-strong hydrogen atom acceptor very strong one-electron donor
	$\Delta H_{H\text{-}A}(GluNA^+) = -74.6$ kcal $\Delta H_{HA}(GluNA^+) = -37.6$ kcal $E_{red}(GluNA^+) = -1.248$ V	not strong hydride acceptor and electrophilic agent poor hydrogen acceptor, weak antioxidant very weak one-electron oxidant

*Note: $\Delta H_{PA}(GluNA^{\bullet})$, $\Delta H_{HA}(GluNA^{\bullet})$, $\Delta H_{H\text{-}A}(GluNA^+)$, and $\Delta H_{HA}(GluNA^+)$ are defined as the enthalpy changes of $GluNA^{\bullet}$ to obtain proton and to obtain hydrogen atom, and the enthalpy changes of $GluNA^+$ to obtain hydride anion and to obtain hydrogen in acetonitrile, respectively. The values are equal to the enthalpy changes of the corresponding opposite species to release proton, to release hydrogen atom, and to release hydride anion in acetonitrile by switching the signs.

$PhXn^+$ to react with $iAscH^-$, the position of the new absorption peak was found not to change at 372 nm, which indicates that the species with absorption at 372 nm should be $iAscH^{\bullet}$ rather than $(G)PhXn^{\bullet}$. It is evident that the finding of the new absorption at 372 nm during the hydride transfer from $iAscH^-$ to $(G)PhXn^+$ clearly indicates that the real mechanism of the hydride transfer should be hydrogen transfer initiated by electron transfer ($e-H^{\bullet}$ multistep mechanism) rather than the concerted hydride transfer in one step (step *c*). Figure 11 gives the reaction coordinate diagram of the hydride transfer from $iAscH^-$ to $PhXn^+$ in dry acetonitrile.

By comparing $\Delta H^{\ddagger}$ and $-T\Delta S^{\ddagger}$ of the hydride transfer from $iAscH^-$ to $(G)PhXn^+$ in step *a* and step *d* (Table 3), it is found that the values of $\Delta H^{\ddagger}$ are generally much larger than those of the corresponding $-T\Delta S^{\ddagger}$ for the hydride transfer in step *a*, indicating the transition state in step *a* does not involve chemical bond formation. This result also supports that step *a* of the hydride transfer should belong to electron transfer, since electron transfer does not involve chemical bond formation, and the entropy change is generally quite small. But, for the reaction in step *d*, the values of $\Delta H^{\ddagger}$ are generally much smaller than those of the corresponding $-T\Delta S^{\ddagger}$, indicating the transition state in step *d* involves formation of a new chemical bond.

Comparison of Kinetic Intrinsic Barrier of $iAscH^-$ and GluNAH as Hydride, Electron, and Hydrogen Atom Donors in Acetonitrile. From the mechanism analysis described above on the hydride transfer from $iAscH^-$ and GluNAH to $(G)PhXn^+$ in acetonitrile, it is clear that the hydride transfer from GluNAH to $(G)PhXn^+$ is a one-step hydride transfer mechanism, but the

Scheme 6. Thermodynamic Analytic Platform on the Mechanism of Hydride Transfer from GluNAH to $PhXn^+$ in Acetonitrile

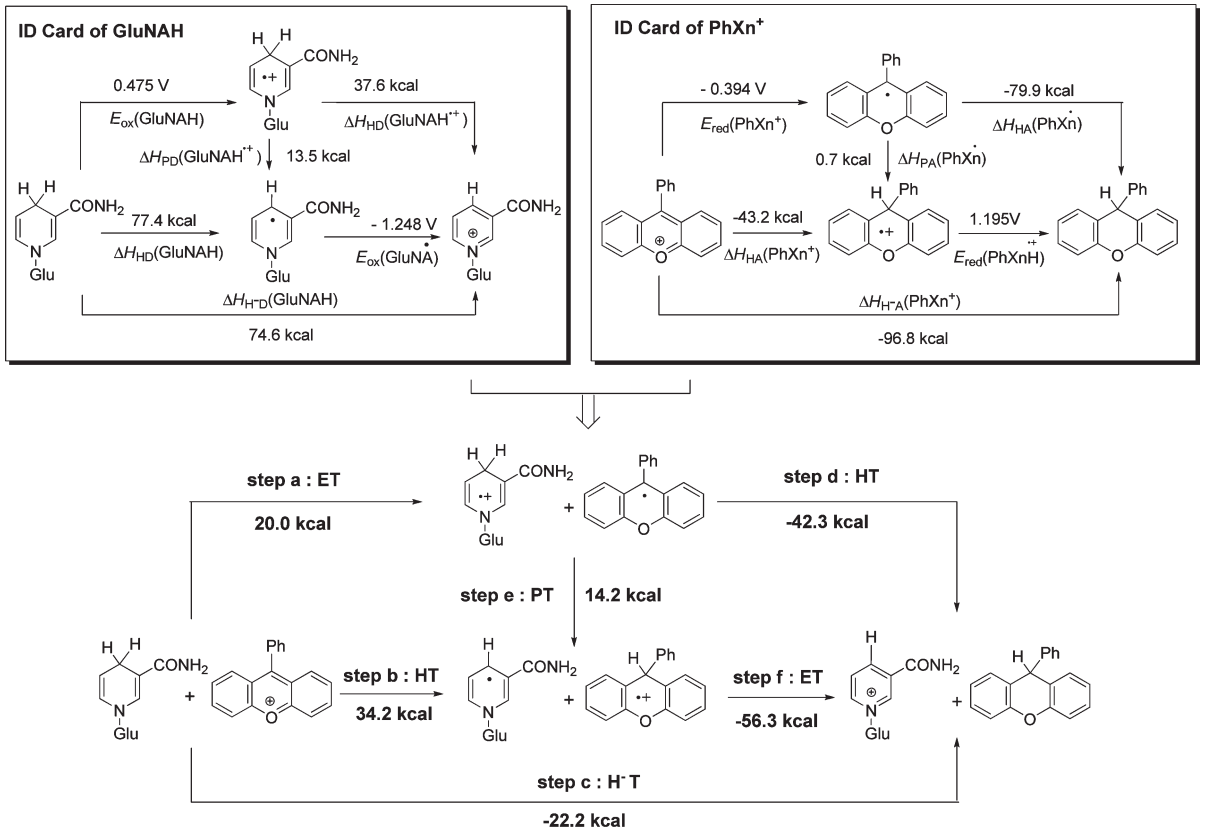

Thermodynamic analytic platform on the mechanism of hydride transfer

hydride transfer from $iAscH^-$ to $(G)PhXn^+$ is multistep rather than a one-step mechanism. For the hydride transfer from GluNAH to $(G)PhXn^+$, the one-step hydride transfer mechanism is not difficult to comprehend, since the thermodynamic driving force of the one-step hydride transfer is much larger than those of the initial electron transfer and the initial hydrogen atom transfer. But, for the hydride transfer from $iAscH^-$ to $(G)PhXn^+$, there are at least two questions which are worthy of asking: (1) Why cannot the one step hydride transfer from $iAscH^-$ to $(G)PhXn^+$ take place, although the thermodynamic driving force of the one-step hydride transfer is much larger than that of the initial electron transfer and the hydrogen atom transfer? (2) Why is the rate of the hydrogen atom transfer in the second step much lower than that of the initial electron transfer, although the thermodynamic driving force of the hydrogen atom transfer is much larger than that of the initial electron transfer? In order to answer those questions, the kinetic intrinsic barrier energy of the related chemical processes needs examination, since a chemical reaction rate is not only dependent on the thermodynamic driving force of the reaction but also dependent on the intrinsic barrier energy of the reaction. In order to estimate the intrinsic barrier energy of the each reaction step of hydride transfer from $iAscH^-$ and GluNAH to $(G)PhXn^+$ in acetonitrile, Brønsted–Evans–Polanyi relations on the each step reaction of the hydride transfer from $iAscH^-$ and GluNAH to $(G)PhXn^+$ in acetonitrile were examined (Figures 12–15).

From Figure 12, it is clear that the Brønsted–Evans–Polanyi relation for the hydride transfer from GluNAH to $(G)PhXn^+$ in step *c* is linear, and the line slope is 0.360 and the line intercept is 19.4 kcal/mol. The line intercept in Figure 12 is the value of the activation free energy ($\Delta G^{\ddagger}$) of the hydride transfer from GluNAH to $(G)PhXn^+$ when the thermodynamic driving force (ΔH_{rxn}) is equal to zero. According to the definition of intrinsic barrier energy of a reaction that the intrinsic barrier energy of a reaction is defined as the activation free energy ($\Delta G^{\ddagger}$) of the reaction when the thermodynamic driving force of the reaction is zero,[61] it is clear that the line intercept value (19.4 kcal/mol) in Figure 12 is just the kinetic intrinsic barrier energy ($\Delta G_0^{\ddagger}$) of the hydride transfer from GluNAH to $(G)PhXn^+$ in acetonitrile.

However, for the kinetic intrinsic barrier energy of the hydride transfer from $iAscH^-$ to $(G)PhXn^+$ in acetonitrile, the detailed value cannot be directly derived from the Brønsted–Evans–Polanyi relation for the hydride transfer from $iAscH^-$ to $(G)PhXn^+$ in one step like the case of the hydride transfer from GluNAH to $(G)PhXn^+$, since the real mechanism of the hydride transfer from $iAscH^-$ to $(G)PhXn^+$ is not a hydride one-step transfer. In order to infer the intrinsic barrier energy of the hydride transfer from $iAscH^-$ to $(G)PhXn^+$ in acetonitrile, the hydride transfer from $iAscH^-$ to $(G)PhXn^+$ in acetonitrile might be considered as the pseudoconcerted hydride transfer in one step as shown in Figure 11 (red line). It is clear that, when the Brønsted–Evans–Polanyi relations on the pseudoconcerted hydride transfer from $iAscH^-$ to $(G)PhXn^+$ in acetonitrile were examined, a good linear plot of the activation free energy against thermodynamic driving force ΔH_{rxn} for the pseudoconcerted

dx.doi.org/10.1021/jp2067974 |*J. Phys. Chem. B* 2011, 115, 14794–14811

Scheme 7. Thermodynamic Analytic Platform on the Mechanism of Hydride Transfer from $iAscH^-$ to $PhXn^+$ in Acetonitrile

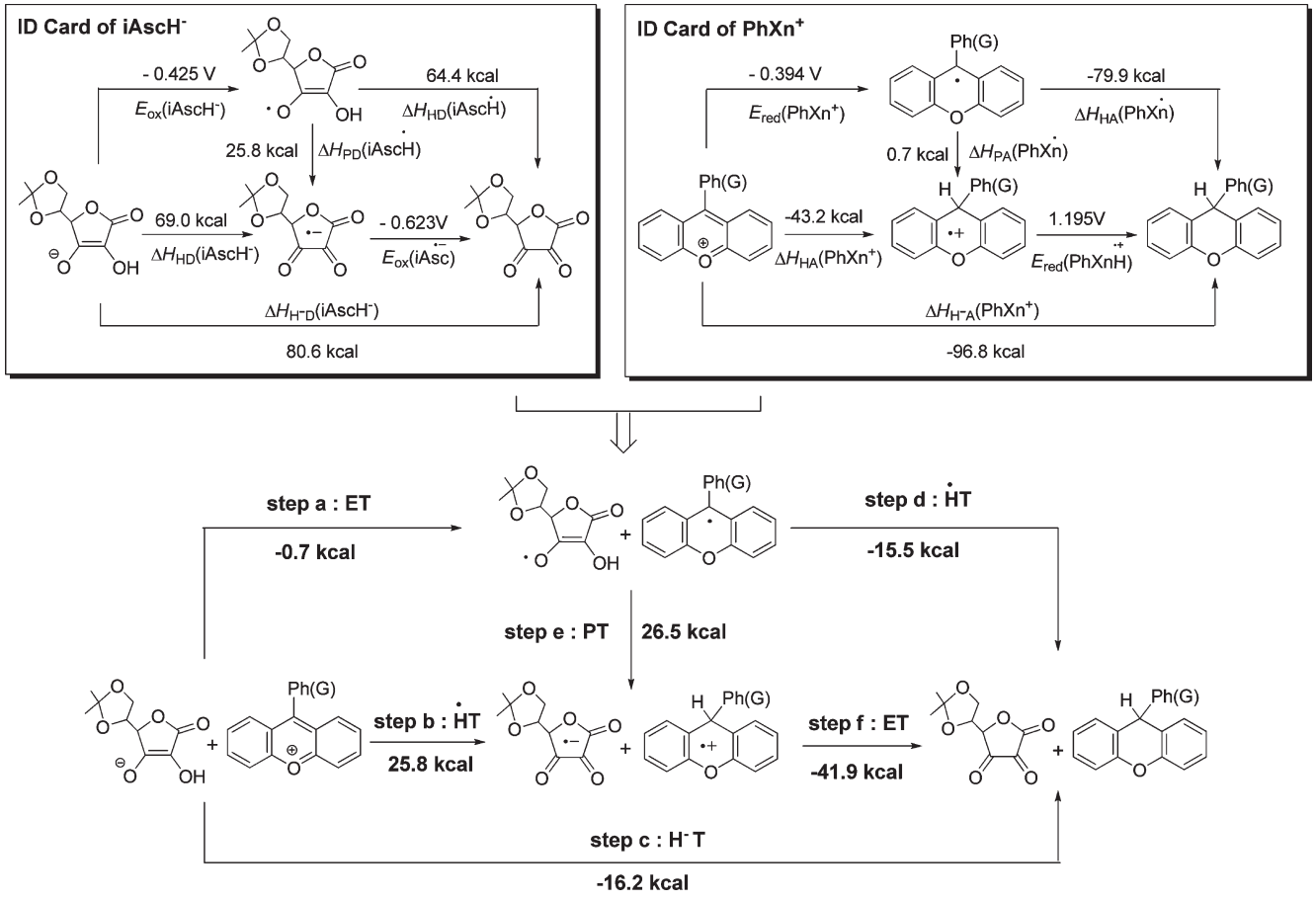

Thermodynamic analytic platform on the mechanism of hydride transfer

hydride transfer (i.e., step *c*) was obtained (Figure 13) and the line slope is 0.760 and the line intercept is 26.3 kcal/mol. The intrinsic barrier energy of the formal (pseudoconcerted) hydride transfer from $iAscH^-$ to $(G)PhXn^+$ in acetonitrile is 26.3 kcal/mol, which is larger than of the hydride transfer from GluNAH to $PhXn^+$ in acetonitrile (19.4 kcal/mol) by 6.9 kcal/mol. Since the intrinsic barrier energy of the formal hydride transfer from $iAscH^-$ to $(G)PhXn^+$ in acetonitrile is larger than that of the hydride transfer from GluNAH to $(G)PhXn^+$ by 6.9 kcal/mol and thermodynamic driving force of the hydride transfer from $iAscH^-$ to $(G)PhXn^+$ in acetonitrile is smaller than that of the hydride transfer from GluNAH to $(G)PhXn^+$ by 6.0 kcal/mol, we can make a conclusion that GluNAH is a good hydride donor, but $iAscH^-$ is not a good hydride donor; the mechanism of hydride transfer from GluNAH generally is a one step, but the mechanism of hydride transfer from $iAscH^-$ generally needs multiple steps; i.e., in most cases, the concerted hydride transfer from $iAscH^-$ could be forbidden.

In the same way, the intrinsic barrier energy of the initial electron transfer from $iAscH^-$ to $(G)PhXn^+$ in step *a* and the intrinsic barrier energy of the followed hydrogen atom transfer from $iAscH^•$ to $(G)PhXn^•$ in step *d* all can be obtained from the line intercept (11.1 kcal/mol) in Figure 14 and from the line intercept (17.0 kcal/mol) in Figure 15. By comparing the intrinsic barrier energies of the initial electron transfer from $iAscH^-$ to $(G)PhXn^+$ in step *a* (11.1 kcal/mol) and the followed hydrogen atom transfer from $iAscH^•$ to $(G)PhXn^•$ (17.0 kcal/mol), it is found that the intrinsic barrier energy of the initial electron transfer in step *a* (11.1 kcal/mol) is smaller than that of the following hydrogen transfer (17.0 kcal/mol) by 5.9 kcal/mol, which can be used to understand why the hydrogen-transfer reaction in the second step is the rate determined, although the thermodynamic driving force of the hydrogen transfer is much larger than that of the initial electron transfer. In the same way, it is not difficult to understand why the hydride transfer from $iAscH^-$ to $(G)PhXn^+$ chose the electron transfer initiated multistep mechanism rather than the concerted hydride transfer one-step mechanism; the reason is that the intrinsic barrier energies of the concerted hydride transfer from $iAscH^-$ to $(G)PhXn^+$ in acetonitrile (26.3 kcal/mol) are larger than those of the corresponding electron transfer from $iAscH^-$ to $(G)PhXn^+$ in acetonitrile (11.1 kcal/mol) by 15.2 kcal/mol, although the thermodynamic driving force of the concerted hydride transfer is much larger than that of the electron transfer.

Comparison of the Character of Transition States of the Related Reactions with GluNAH and $iAscH^-$ as Hydride, Electron and Hydrogen Atom Source. Although the thermodynamic diving force, intrinsic barrier energy, and mechanism of GluNAH and $iAscH^-$ as hydride, hydrogen atom, and electron donors have been compared in detail, the transition structures of

dx.doi.org/10.1021/jp2067974 |J. Phys. Chem. B 2011, 115, 14794–14811

Table 8. Energetics of Each Mechanistic Step of Hydride Transfer from iAscH$^-$ and GluNAH to (G)PhXn$^+$ in Acetonitrile Shown in Schemes 6 and 7 (kcal/mol)

	ΔG (or ΔH) (kcal/mol)					
(G)PhXn$^+$	step a[a]	step b[b]	step c[c]	step d[d]	step e[e]	step f[f]
For Hydride Transfer from GluNAH to (G)PhXn$^+$						
p-CF_3	18.7	33.7	−24.1	−42.8	14.9	−57.8
m-CF_3	18.9	33.7	−23.7	−42.6	14.8	−57.4
p-Cl	19.1	33.6	−23.3	−42.5	14.5	−56.9
p-Br	19.3	33.7	−23.0	−42.3	14.4	−56.6
m-OCH_3	19.7	33.8	−22.7	−42.5	14.2	−56.5
p-H	20.0	34.2	−22.2	−42.3	14.2	−56.3
m-CH_3	20.4	34.4	−21.8	−42.2	14.0	−56.2
p-CH_3	20.5	34.5	−21.4	−41.9	14.0	−55.9
p-OCH_3	20.9	34.8	−20.9	−41.8	13.8	−55.6
For Hydride Transfer from iAscH$^-$ to (G)PhXn$^+$						
p-CF_3	−2.1	25.3	−18.1	−16.0	27.3	−43.4
m-CF_3	−1.9	25.3	−17.7	−15.8	27.2	−43.0
p-Cl	−1.6	25.2	−17.3	−15.7	26.9	−42.5
p-Br	−1.5	25.3	−17.0	−15.6	26.8	−42.2
m-OCH_3	−1.2	25.4	−16.7	−15.5	26.4	−42.1
p-H	−0.7	25.8	−16.2	−15.5	26.5	−41.9
m-CH_3	−0.4	26.0	−15.8	−15.4	26.4	−41.8
p-CH_3	−0.3	26.1	−15.4	−15.1	26.4	−41.5
p-OCH_3	0.1	26.4	−14.9	−15.0	26.2	−41.2

[a] Derived from the equation $\Delta G(\text{step a}) = -23.06\{E_{red}[(G)PhXn^+] - E_{ox}(XH)\}$, XH = iAscH$^-$ and GluNAH. [b] Derived from the equation $\Delta H(\text{step b}) = \Delta H_{HD}(XH) - \Delta H_{HD}[(G)PhXnH^\bullet]$. [c] Derived from the equation: $\Delta H(\text{step c}) = \Delta H_{H^-D}(XH) - \Delta H_{H^-D}[(G)PhXnH]$. [d] Derived from the equation: $\Delta H(\text{step d}) = \Delta H_{HD}(XH^{\bullet+}) - \Delta H_{HD}[(G)PhXnH]$. [e] Derived from the equation: $\Delta H(\text{step e}) = \Delta H_{PD}(XH^{\bullet+}) - \Delta H_{PD}[(G)PhXn^{\bullet+}]$. [f] Derived from the equation: $\Delta G(\text{step f}) = -23.06\{E_{ox}[(G)PhXnH] - E_{ox}(X^\bullet)\}$.

the related reactions are not clear. To quantitatively elucidate the structural characters of the transition states (such as bond energies and bond lengths of the forming or breaking chemical bonds), the effective charge changes on the reaction center atoms (C_4 for GluNAH and C_9 for PhXn$^+$) in the transition states were estimated.

For the effective charge change on the C_9 atom in (G)PhXn$^+$ from the (G)PhXn$^+$ in the reaction initial state to the "H--PhXn" in the transition state, the effective charge on C_9 in the transition state can be estimated by using Hammett-type linear free energy analysis method, since the Hammett linear free-energy relationship analysis can provide a very efficient access to estimate the effective charge distribution.[34b] Figure 16 shows the plots of the activation Gibbs free energy change ($\Delta G^{\ddagger}$) and the thermodynamic driving force (ΔH_{rxn}) of the hydride transfer from GluNAH to (G)PhXn$^+$ against the Hammett substituent constant σ. From Figure 16, two excellent straight lines with the line slopes of -1.43 ± 0.05 (equivalent to ρ of 0.25)[62] for the process from the reactants to the transition state, and -3.91 ± 0.14 (equivalent to ρ of 0.69)[62] for the hydride transfer from GluNAH to (G)PhXn$^+$ to form GluNA$^+$ and (G)PhXnH are observed, which means that Hammett linear free energy relationship holds in the two chemical processes. According to the nature of Hammett

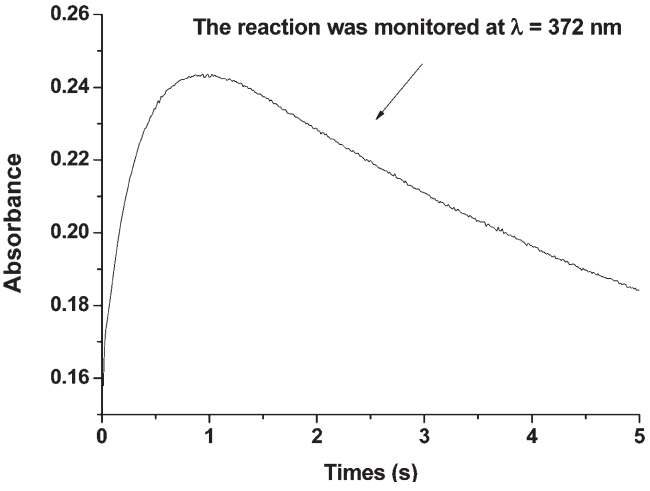

Figure 9. UV−vis spectra change at λ = 372 nm for the reaction of iAscH$^-$ (1×10^{-2} M) with PhXn$^+$ (4×10^{-4} M) in dry acetonitrile at 298 K over the course of 5 s.

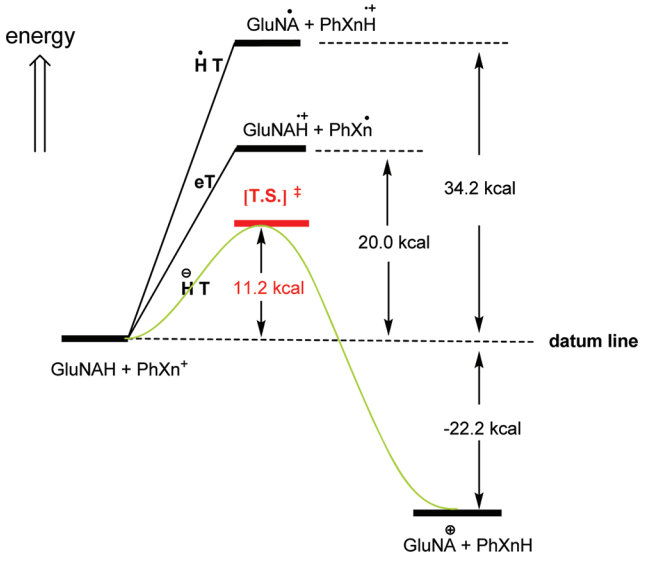

Figure 10. Comparison of state energy changes for the three possible initial steps of the hydride transfer from GluNAH to PhXn$^+$ and the activation free energy of the hydride transfer.

substituent effect, it is conceived that the sign of the line slope values reflects increase or decrease of the effective charge on the carbon (C_9) atom in the pyran ring, and the magnitude of the line slope values is a measurement of the effective charge change on the C_9 atom during the corresponding reaction processes.[63] In order to quantitatively evaluate the relative effective charge changes on the C_9 atom in (G)PhXn$^+$ from the (G)PhXn$^+$ in the reaction initial state to the (G)PhXn$^+$ in the transition state, we defined that the effective charges on the C_9 atom in the free (G)PhXnH and in the free (G)PhXn$^+$ are zero and positive one (+1) unit, respectively. This definition indicates that the negative line slope of −3.91 for the hydride transfer from GluNAH to (G)PhXn$^+$ to form GluNA$^+$ and (G)PhXnH is equivalent to the negative effective charge increase of one unit (−1.000) on the C_9 atom from (G)PhXn$^+$ to (G)PhXnH. According to this relationship, it is easy to deduce that the line slope of −1.43 for the formation of the transition state is equivalent to the

dx.doi.org/10.1021/jp2067974 |J. Phys. Chem. B 2011, 115, 14794–14811

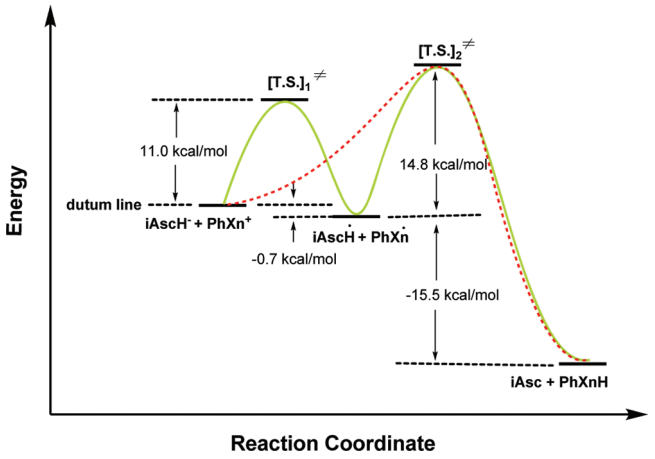

Figure 11. Reaction coordinate diagram of hydride transfer from $iAscH^-$ to $PhXn^+$ in dry acetonitrile: (1) real pathway of hydride transfer from $iAscH^-$ to $PhXn^+$ (green volcano curve); (2) hypothetical one-step mechanism hydride transfer from $iAscH^-$ to $PhXn^+$ (red volcano curve).

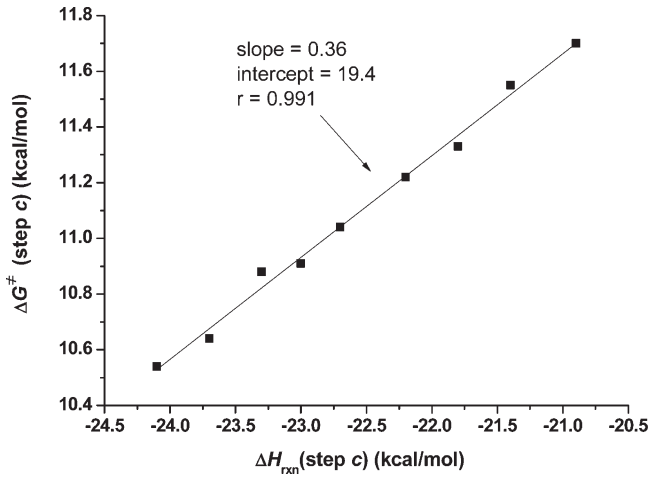

Figure 12. Brønsted−Evans−Polanyi relation for hydride transfer from GluNAH to $(G)PhXn^+$ in step c.

negative effective charge increase of 0.366 on the C_9 atom from the free $(G)PhXn^+$ as the reactant to the $(G)PhXn^+$ moiety in the transition state. Since the effective charge on the C_9 atom in free $(G)PhXn^+$ has been defined as positive one (+1.000) unit, the effective charge on the C_9 atom in the transition state should be +0.634 unit (eq 12), which means that $(G)PhXn^+$ gets negative charge of −0.366 unit in going from the reaction initial state to the transition state. Since the C_9−H bond formation energy of PhXnH is −96.8 kcal/mol in acetonitrile and corresponds to the effective charge increase of −1.000 unit on the C_9 atom in the C_9−H bond formation process, $PhXn^+ + H^- \rightarrow PhXnH$, it is conceived that the formation energy of "C_9--H bond" in the transition state should be −35.4 kcal/mol. In addition, from Hooke's law we derive the relationship of C_9−H bond length and C_9−H bond energy: $\Delta r = (2\Delta\Delta H/k)^{1/2}$, in which Δr is the bond length change of C_9−H, $\Delta\Delta H$ is bond energy change of C_9−H, and k is bond harmonic force constant of C_9−H, the value is about 513.2 kcal mol^{-1} $Å^{-2}$ (in acetonitrile).[64] According to the formula, the C_9--H bond length in the transition state can be estimated. The result is 0.159 nm in acetonitrile.

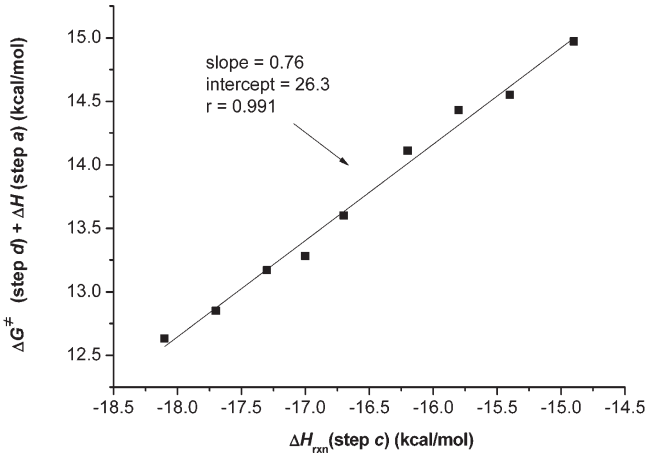

Figure 13. Brønsted−Evans−Polanyi relation of the formal hydride transfer from $iAscH^-$ to $(G)PhXn^+$ in step c.

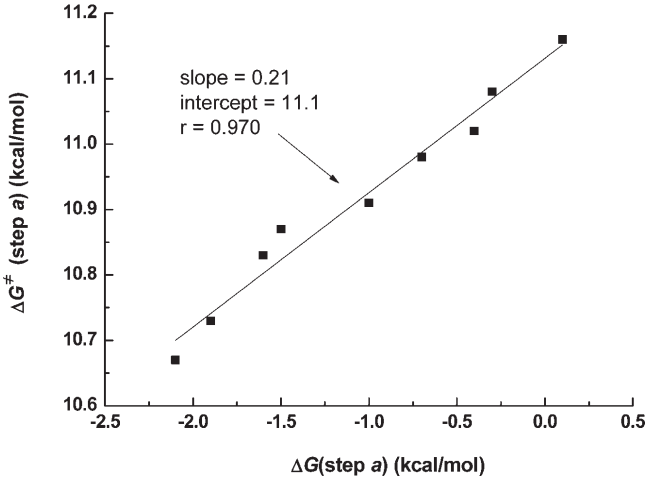

Figure 14. Brønsted−Evans−Polanyi relation of electron transfer from $iAscH^-$ to $(G)PhXn^+$ (step a) in acetonitrile.

For the effective charge change on the C_4 atom in GluNAH in going from GluNAH to the "GluNA--H" in the transition state, the following strategy can be used to estimate it. According to Eyring theory about the transition state, the Gibbs activation free energy of hydride transfer from GluNAH to $PhXn^+$ (11.2 kcal/mol) is equal to the sum of the formation enthalpy of "H--PhXn bond" in the transition state $[GluNA\text{--}H\text{--}PhXn]^{‡}$ and the activation enthalpy of "GluNA--H bond" in the transition state. Since the formation enthalpy of "H--C_9 bond" in the transition state (−35.4 kcal/mol) can be estimated according to the effective charge change (−0.366) on the C_9 atom in $(G)PhXn^+$ going from the reaction initial state to the transition state, the activation energy of "C_4--H bond" in the transition state should be 46.6 kcal/mol, i.e., the heterolytic dissociation energy of C_4--H in the transition state is 74.6 − 46.6 = 28.0 kcal/mol. Since the effective charge increase of one unit (+1.000) on the C_4 atom in GluNAH going from GluNAH to $GluNA^+$ is equivalent to the C_4−H bond heterolytic dissociation energy (74.6 kcal/mol), the effective positive charge increase on the C_4 atom in GluNAH going from the reaction initial state to the transition state should be +0.625. On the basis of the definition of the effective charge (0.000) on the C_4 atom of GluNAH in the reaction initial state, the effective positive charge on the C_4 atom in

dx.doi.org/10.1021/jp2067974 |J. Phys. Chem. B 2011, 115, 14794–14811

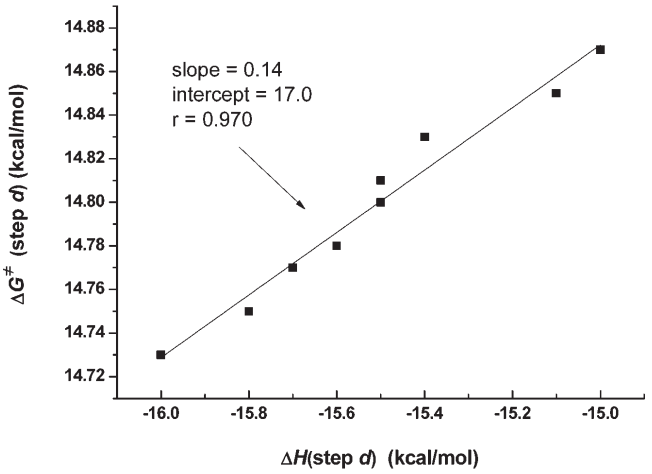

Figure 15. Brønsted−Evans−Polanyi relation of the hydrogen atom transfer from iAscH$^{\bullet}$ to (G)PhXn$^{\bullet}$ in step d.

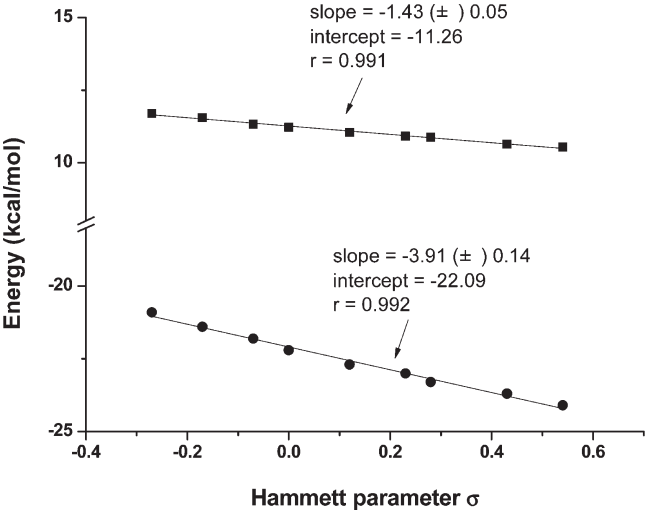

Figure 16. Hammett plots of $\Delta G^{\ddagger}$ (■) and ΔH_{rxn} (●) for hydride transfer from GluNAH to (G)PhXn^{+} in acetonitrile vs σ.

the transition state can be easily estimated (+0.625). From the effective charges on the C_4 atom (+0.625) and the C_9 atom (+0.634) in the transition state, it is not difficult to get that the transferring hydride anion in the transition state carries an effective charge of −0.259 unit. Since the bond energy of C_4−H in the transition state is 28.0 kcal/mol, the bond energy of C_4−H in the transition state can be evaluated according to the same method as used for C_9−H bond length in the transition state. The result is 0.143 nm. The effective charges on the reaction center atoms (C_4 and C_9), bond energies, and bond length of C_4−H and C_9−H in the transition state for the hydride transfer from GluNAH to PhXn^{+} in acetonitrile are given in eq 12.

By using the same strategy, the effective charges on the O_3 in iAscH^{-} and on the C_9 in PhXn^{+} in the transition states for the electron transfer from iAscH^{-} to PhXn^{+} in the initial step and for the hydrogen atom transfer from iAscH$^{\bullet}$ to PhXn$^{\bullet}$ in the second step as well as for the formal hydride one-step transfer from iAscH^{-} to PhXn^{+} all can be estimated according to the related line slopes in the plots of activation Gibbs free energy change ($\Delta G^{\ddagger}$) and thermodynamic driving force of the electron transfer,

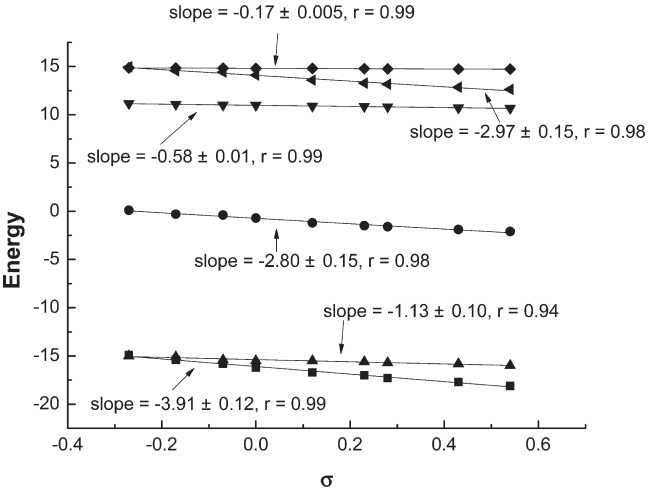

Figure 17. Hammett plots of ΔH(step c) (■), ΔH(step d)(▲), ΔG(step a) (●), $\Delta G^{\ddagger}$(step c) (◀), $\Delta G^{\ddagger}$(step d) (◆), and $\Delta G^{\ddagger}$(step a) (▼) for hydride transfer from iAscH^{-} to (G)PhXn^{+} in acetonitrile vs σ.

hydrogen atom transfer, and the formal hydride transfer against the Hammett substituent constant σ (Figure 17); the results also are shown in eqs 13, 14, and 15, respectively. The bond energies of O_3−H and C_9−H in the related transition state are estimated according to the effective charge change on the reaction center atoms (O_3 for iAscH^{-} and C_9 for PhXnH) and the corresponding O_3−H and C_9−H bond energies for iAscH^{-} and PhXnH at ground states in acetonitrile, and the results also are given in eqs 13−15, respectively.

For the reaction of hydride transfer from GluNAH to PhXn^{+} in CH_3CN:

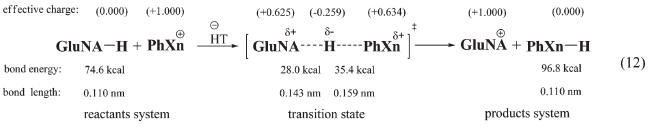

(12)

For the reaction of electron transfer from iAscH^{-} to PhXn^{+} in CH_3CN:

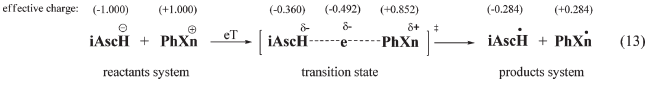

(13)

For the reaction of hydrogen atom transfer from iAscH$^{\bullet}$ to PhXn$^{\bullet}$ in CH_3CN:

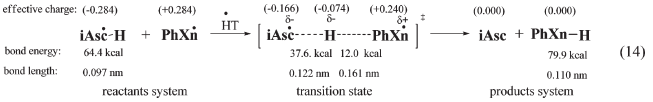

(14)

For the reaction of the formal hydride transfer from iAscH^{-} to PhXn^{+} in CH_3CN:

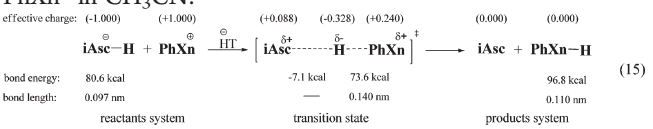

(15)

From the transition state of hydride transfer from GluNAH to PhXn^{+} in eq 12, the following results can be found: (1) The distance between two reaction center atoms is 0.302 nm, which is much larger than the sum of the two C−H bond length (0.220 nm), but smaller than the sum of the van der Waals

dx.doi.org/10.1021/jp2067974 |J. Phys. Chem. B 2011, 115, 14794–14811

Scheme 8. Thermodynamic Analytic Platform on the Possible Reactions of the Members between GluNAH Family and iAsc Family in Acetonitrile

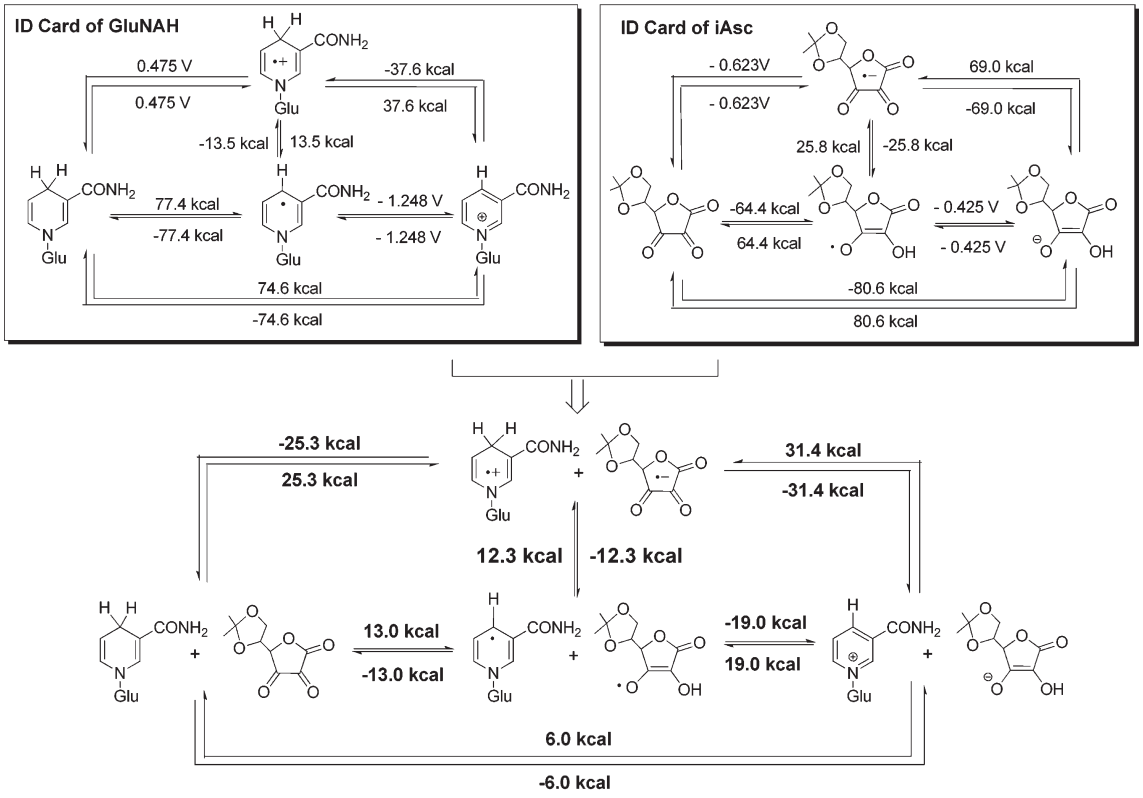

Thermodynamic analytic platform on the possible reactions between GluNAH family and iAsc family

radius of the two reaction center carbon atoms (0.340 nm), indicating that the valence bond orbital of the two reaction center atoms could slightly overlap; i.e., the transition state of the hydride transfer could be triangular rather than linear. (2) The C_4—H bond length (0.143 nm) is shorter than that of C_9—H bond length (0.159 nm), meaning that the transition state is more similar to the reactants than to the products. (3) The transferred hydrogen atom carried the charge of −0.259, meaning that the dissociation of C_4—H bond and the formation of C_9—H bond is not synchro percentage conversion before reaching the transition state, and the degree of the C_4—H bond dissociation is larger than that of the C_9—H bond formation. From the transition state of the formal hydride transfer from $iAscH^-$ to $PhXn^+$ (eq 15), it is clear that the effective charge of the center carbon atom is positive (+0.088), which is evidently unreasonable. This result also further indicates that the hydride transfer from $iAscH^-$ to $PhXn^+$ actually is not completed by one step.

Diagnoses of Possible Reactions of the Members between the $iAscH^-$ Family and the GluNAH Family. Since $AscH^-$ and NADH are two important bioreductants and the hydride transfer from $AscH^-$ and NADH could involve multistep mechanism, it is conceived that $AscH^-$ and NADH as well as their various reaction intermediates all could coexist in living body. In order to infer the possible reactions between $AscH^-$ and NADH as well as their various reaction intermediates in vivo, a mimic thermodynamic analysis platform on the likely reactions among them was constructed according to Molecule ID Cards of iAsc and GluNAH in acetonitrile (Scheme 8). From Scheme 8, the following predictions on the reactions between the members of $iAscH^-$ family and GluNAH family can be made: (i) When iAsc and GluNAH are mixed in acetonitrile, hydride and hydrogen transfers are allowed from GluNAH to iAsc to yield $GluNA^+$ and $iAscH^-$ or $GluNA^•$ and $iAscH^•$, respectively, but electron transfer is forbidden. (ii) When neutral radical $iAscH^•$ and cation radical $GluNAH^{•+}$ contacted each other in acetonitrile, $iAscH^-$ and $GluNA^+$, $iAsc^{•-}$ and $GluNA^•$, and iAsc and GluNAH could be formed by hydrogen, proton, and electron transfers, respectively. (iii) When $iAsc^{•-}$ and $GluNA^•$ met together in acetonitrile, $iAscH^-$ and GluNAH as well as iAsc and GluNAH could be formed by hydrogen and electron transfers, respectively, but proton transfer is forbidden. (iv) When $iAscH^-$ and $GluNA^+$ were mixed in acetonitrile, no reaction was allowed. Among the four couples of the reaction partners, the couple of $iAscH^-$ and $GluNA^+$ is the most stable reaction partner, but the couple of $iAscH^•$ and $GluNAH^{•+}$ is the most active reaction partner. It is evident that these diagnoses should be useful for our understanding and interpretation of the real reduction mechanism of dehydroascorbic acid by NADH in vivo.

■ CONCLUSIONS

In this work, 5,6-isopropylidene ascorbate ($iAscH^-$) and β-D-glucopyranosyl-1,4-dihydro- nicotinamide acetate (GluNAH) were synthesized as ascorbate ($AscH^-$) and dihydronicotinamide adenine dinucleotide (NADH) models. After the thermodynamics, kinetics, and mechanism of $iAscH^-$ and GluNAH as hydride, hydrogen atom, and electron sources to react with the corresponding form of the substituted phenylxanthium perchlorate (G)$PhXn^+$ as the reaction partners in acetonitrile were examined and compared in detail, the

following conclusions can be made: (1) $iAscH^-$ is a quite weak hydride donor, but a good one-electron donor. GluNAH is a weak one electron donor, but a good hydride donor. The electron-donating ability of $iAscH^-$ in acetonitrile is larger than that of GluNAH by 0.900 V (equivalent to 20.8 kcal/mol), but the hydride-donating ability of $iAscH^-$ in acetonitrile is smaller than that of GluNAH by 6.0 kcal/mol, which means that GluNAH is a good two-electron (or hydride anion) donor, and $iAscH^-$ is a good single electron donor. (2) $iAscH^-$ is a good hydrogen atom donor, but GluNAH is a weak hydrogen atom donor; the hydrogen-donating ability of $iAscH^-$ in acetonitrile is larger than that of GluNAH by 8.4 kcal/mol, which suggests that $iAscH^-$ is a good antioxidant, but GluNAH cannot be used as antioxidant. (3) $iAscH^-$ as hydride source generally adopts multistep hydride-transfer mechanism initiated by electron transfer, but GluNAH as hydride source generally adopts one-step hydride-transfer mechanism. (4) Intrinsic energy of $iAscH^-$ as hydride source is much larger than that of GluNAH in acetonitrile; the difference is 6.9 kcal/mol, which also further suggests $iAscH^-$ is not a good hydride donor. (5) As hydrogen atom donor or as antioxidant, the mechanism of $iAscH^-$ to release hydrogen atom is generally multistep, and in the most cases, the hydrogen atom transfer was initiated by electron transfer. Since the structure of GluNAH is quite close to the redox active center structure of NADH, and the structure of $iAscH^-$ is quite close to the redox active center structure of $AscH^-$, as well as the polarity of acetonitrile is quite close to that of peptide bond in proteins, it is evident that these important experimental results can be used to well answer the title question: what are the differences of ascorbic acid and NADH as electron and hydride sources in vivo on thermodynamics, kinetics, and mechanism?

AUTHOR INFORMATION

Corresponding Author

*E-mail: xqzhu@nankai.edu.cn.

ACKNOWLEDGMENT

Financial support from the National Natural Science Foundation of China (Grant Nos. 21072104, 20921120403, and 20832004), the Ministry of Science and Technology of China (Grant No. 2004CB719905), and the 111 Project (B06005) is gratefully acknowledged.

REFERENCES

(1) (a) *Vitamin C in Health and Disease*; Packer, L., Fuchs, J., Eds.; Marcel Dekker: New York, 1997; Vol. 5. (b) Kroneck, P. M. H.; Armstrong, F. A.; Merkle, H.; Marchesini, A. Ascorbate oxidase: molecular properties and catalytic activity. In *Ascorbic Acid: Chemistry, Metabolism and Uses*; Seib, P. A., Tolbert, B. M., Eds.; Advances in Chemistry Series 200; American Chemical Society: Washington, DC, 1982; pp 223−248. (c) Neta, P. *Chem. Rev.* **1972**, *72*, 533–543. (d) Karrer, P. *Chem. Rev.* **1934**, *14*, 17–30.

(2) (a) Stout, D. M.; Meyers, A. I. *Chem. Rev.* **1982**, *82*, 223–243. (b) Murakami, Y.; Kikuchi, J.-I.; Hisaeda, Y.; Hayashida, O. *Chem. Rev.* **1996**, *96*, 721–758. (c) Eisner, U.; Kuthan, J. *Chem. Rev.* **1972**, *72*, 1–42.

(3) Harnadek, G. J.; Ries, E. A.; Farhat, A.; Njus, D. *J. Biol. Chem.* **1990**, *265*, 18135–18141.

(4) Bisby, R. H.; Parker, A. W. *Arch. Biochem. Biophys.* **1995**, *317*, 170–178.

(5) Isaacs, N. S.; Eldik, R. *J. Chem. Soc., Perkin Trans. 2* **1997**, No. No. 8, 1465–1467.

(6) Bartlett, D.; Church, D.; Bounds, P.; Koppenol, W. H. *Free Radical Biol. Med.* **1995**, *18*, 85.

(7) (a) Nakanishi, N.; Takeuchi, F.; Tsubaki, M. *J. Biochem.* **2007**, *142*, 553–560. (b) Njus, D.; Wigle, M.; Kelley, P. M.; Kipp, B. H.; Schlegel, H. B. *Biochem.* **2001**, *40*, 11905–11911.

(8) Kytzia, A.; Korth, H.-G.; Sustmann, R.; de Groot, H.; Kirsch, M. *Chem.—Eur. J.* **2006**, *12*, 8786–8797.

(9) May, J. M.; Qu, Z. C.; Li, X. *Biochem. Pharmacol.* **2001**, *62*, 873–881.

(10) Nishiyama, I.; Yamashita, Y.; Yamanaka, M.; Shimohashi, A.; Fukuda, T.; Oota, T. *J. Agr. Food. Chem.* **2004**, *52*, 5472–5475.

(11) Gebicki, J.; Marcinek, A.; Zielonka, J. *Acc. Chem. Res.* **2004**, *37*, 379–386.

(12) (a) Styer, L. *Biochemistry*, 3rd ed; Freeman: New York, 1988; Chapter 17. (b) Walsh, C. *Enzymatic Reaction Mechanism*; W. H. Freeman: San Francisco, 1979; Chapter 10. (c) Westheimer, F. H. *Pyridine Nucleotide Coenzyme*; Dolphin, D., Poulson, R., Avramovic, O., Eds.; Wiley-Interscience: New York, 1988; Part A, p 253.

(13) Birrell, J. A.; Yakovlev, G.; Hirst, J. *Biochemistry* **2009**, *48*, 12005–12013.

(14) Yamazaki, S.; Tsai, L. *J. Biol. Chem.* **1980**, *255*, 6462–6465.

(15) Carlson, B. W.; Miller, L. L. *J. Am. Chem. Soc.* **1985**, *107*, 479–485.

(16) (a) *Biochemistry*; Campbell, M. K., Ed.; Saunders College Publishing: London, 1995; pp 285−290. (b) *Nicotinamide Nucleotide Transhydrogenase in the Enzymes*; Rydstorm, J., Hoeck, L., Ernster, Eds.; New York, 1976; pp 76−98.

(17) (a) Silverblatt, E.; Robinson, A. L.; King, C. G. *J. Am. Chem. Soc.* **1943**, *65*, 137–141. (b) Weissberger, A.; LuValle, J. E.; Thomas, D. S. *J. Am. Chem. Soc.* **1943**, *65*, 1934–1939. (c) Weissberger, A.; LuValle, J. E. *J. Am. Chem. Soc.* **1944**, *66*, 700–705.

(18) (a) Fukuzumi, S.; Tanaka, T. *Photoinduced Electron Transfer*; Fox, M. A., Chanon, M., Eds.; Elsevier: Amsterdam, The Netherlands, 1988; Part C, Chapter 10. (b) Fukuzumi, S. *Advances in Electron Transfer Chemistry*; Mariano, P. S., Ed.; JAI Press: Greenwich, CT, 1992; pp 67−175.

(19) Zhu, X.-Q.; Yang, Y.; Zhang, M.; Cheng, J.-P. *J. Am. Chem. Soc.* **2003**, *125*, 15298–15299.

(20) (a) Zielonka, J.; Marcinek, A.; Adamus, J.; Gebicki, J. *J. Phys. Chem. A* **2003**, *107*, 9860–9864. (b) Bartlett, P. N.; Simon, E. *J. Am. Chem. Soc.* **2003**, *125*, 4014–4015.

(21) (a) Gassner, G.; Wang, L.; Batie, C.; Ballou, D. P. *Biochemistry* **1994**, *33*, 12184–12193. (b) Gassner, G. T.; Lippard, S. J. *Biochemistry* **1999**, *38*, 12768–12785. (c) Nivière, V.; Vanoni, M. A.; Zanetti, G.; Fontecave, M. *Biochemistry* **1998**, *37*, 11879–11887.

(22) (a) Choi, H.-I.; Kim, H.-J.; Park, J.-I.; Shin, E.-H.; Kim, D.-W.; Kim, S.-S. *Bioorg. Med. Chem. Lett.* **2009**, *19*, 2079–2082. (b) Spickenreither, M.; Braun, S.; Bernhardt, G.; Dove, S.; Buschauer, A. *Bioorg. Med. Chem. Lett.* **2006**, *16*, 5313–5316.

(23) (a) Pang, J.; Hay, S.; Scrutton, N. S.; Sutcliffe, M. J. *J. Am. Chem. Soc.* **2008**, *130*, 7092–7097. (b) Brondijk, T. H. C.; van Boxel, G. I.; Mather, O. C.; Quirk, P. G.; White, S. A.; Jackson, J. B. *J. Biol. Chem.* **2006**, *281*, 13345–13354.

(24) (a) Bruice, T. C. *Acc. Chem. Res.* **1980**, *13*, 256–262. (b) Walsh, C. *Acc. Chem. Res.* **1980**, *13*, 148–155.

(25) (a) Nisimoto, Y.; Jackson, H. M.; Ogawa, H.; Kawahara, T.; Lambeth, J. D. *Biochemistry* **2010**, *49*, 2433–2442. (b) Afanasyeva, M. S.; Taraban, M. B.; Purtov, P. A.; Leshina, T. V.; Grissom, C. B. *J. Am. Chem. Soc.* **2006**, *128*, 8651–8658. (c) Juarez, O.; Morgan, J. E.; Barquera, B. *J. Biol. Chem.* **2009**, *284*, 8963–8972.

(26) (a) Warren, J. J.; Mayer, J. M. *J. Am. Chem. Soc.* **2010**, *132*, 7784–7793. (b) Warren, J. J.; Mayer, J. M. *J. Am. Chem. Soc.* **2008**, *130*, 2774–2776. (c) Warren, J. J.; Mayer, J. M. *J. Am. Chem. Soc.* **2008**, *130*, 7546–7547.

(27) (a) Sajenko, I.; Pilepic, V.; Brala, C. J.; Ursic, S. *J. Phys. Chem. A* **2010**, *114*, 3423–3430. (b) Vuina, D.; Pilepic, V.; Ljubas, D.; Sankovic, K.; Sajenko, I.; Ursic, S. *Tetrahedron Lett.* **2007**, *48*, 3633–3637.

(28) De Biase, P. M.; Turjanski, A. G.; Estrin, D. A.; Doctorovich, F. *J. Org. Chem.* **2005**, *70*, 5790–5798.

(29) Chatterjee, D.; Sengupta, A.; Mitra, A.; Basak, S. *Inorg. Chem. Commun.* **2006**, *9*, 1219–1222.

(30) Prieto, F.; Coles, B. A.; Compton, R. G. *J. Phys. Chem. B* **1998**, *102*, 7442–7447.

(31) (a) Fukuzumi, S.; Fujioka, N.; Kotani, H.; Ohkubo, K.; Lee, Y.-M.; Nam, W. *J. Am. Chem. Soc.* **2009**, *131*, 17127–17134. (b) Yuasa, J.; Yamada, S.; Fukuzumi, S. *J. Am. Chem. Soc.* **2008**, *130*, 5808–5820. (c) Fukuzumi, S.; Kotani, H.; Lee, Y.-M.; Nam, W. *J. Am. Chem. Soc.* **2008**, *130*, 15134–15142. (d) Yuasa, J.; Yamada, S.; Fukuzumi, S. *J. Am. Chem. Soc.* **2006**, *128*, 14938–14948. (e) Yuasa, J.; Fukuzumi, S. *J. Am. Chem. Soc.* **2006**, *128*, 14281–14292.

(32) (a) Fukuzumi, S.; Yuasa, J.; Suenobu, T. *J. Am. Chem. Soc.* **2002**, *124*, 12566–12573. (b) Fukuzumi, S.; Ohkubo, K.; Okamoto, T. *J. Am. Chem. Soc.* **2002**, *124*, 14147–14155. (c) Fukuzumi, S.; Fujii, Y.; Suenobu, T. *J. Am. Chem. Soc.* **2001**, *123*, 10191–10199. (d) Fukuzumi, S.; Koumitsu, S.; Hironaka, K.; Tanaka, T. *J. Am. Chem. Soc.* **1987**, *109*, 305–316.

(33) Matsuo, T.; Mayer, J. M. *Inorg. Chem.* **2005**, *44*, 2150–2158.

(34) (a) Zhu, X.-Q.; Zhang, J.-Y.; Cheng, J.-P. *J. Org. Chem.* **2006**, *71*, 7007–7015. (b) Zhu, X.-Q.; Cao, L.; Liu, Y.; Yang, Y.; Lu, J.-Y.; Wang, J.-S.; Cheng, J.-P. *Chem.—Eur. J.* **2003**, *9*, 3937–3945. (c) Zhu, X.-Q.; Li, H.-R.; Li, Q.; Ai, T.; Lu, J.-Y.; Yang, Y.; Cheng, J.-P. *Chem.—Eur. J.* **2003**, *9*, 871–880. (d) Zhu, X.-Q.; Liu, Y.; Zhao, B.-J.; Cheng, J.-P. *J. Org. Chem.* **2001**, *66*, 370–375. (e) Zhu, X.-Q.; Zou, H.-L.; Yuan, P.-W.; Liu, Y.; Cao, L.; Cheng, J.-P. *J. Chem. Soc., Perkin Trans. 2.* **2000**, No. No. 9, 1857–1861. (f) Zhu, X.-Q.; Zhao, B.-J.; Cheng, J.-P. *J. Org. Chem.* **2000**, *65*, 8158–8163. (g) Zhao, B.; Zhu, X.; Lu, Y.; Xia, C.-Z.; Cheng, J.-P. *Tetrahedron Lett.* **2000**, *41*, 257–260. (h) Cheng, J.-P.; Lu, Y.; Zhu, X.-Q.; Sun, Y.-K.; Bi, F.; He, J.-Q. *J. Org. Chem.* **2000**, *65*, 3853–3857. (i) Zhu, X.-Q.; Liu, Y.-C.; Cheng, J.-P. *J. Org. Chem.* **1999**, *64*, 8980–8981.

(35) (a) Kil, H. J.; Lee, I. S. H. *J. Phys. Chem. A* **2009**, *113*, 10704–10709. (b) Lee, I. S. H.; Kil, H. J.; Ji, Y. R. *J. Phys. Org. Chem.* **2007**, *20*, 484–490. (c) Lee, I. S. H.; Ji, Y. R.; Jeoung, E. H. *J. Phys. Chem. A* **2006**, *110*, 3875–3881. (d) Lee, I. S. H.; Chow, K. H.; Kreevoy, M. M. *J. Am. Chem. Soc.* **2002**, *124*, 7755–7761. (e) Lee, I. S. H.; Jeoung, E. H.; Kreevoy, M. M. *J. Am. Chem. Soc.* **2001**, *123*, 7492–7496. (f) Lee, I. S. H.; Jeoung, E. H. *J. Org. Chem.* **1998**, *63*, 7275–7279. (g) Kreevoy, M. M.; Kotchevar, A. T. *J. Am. Chem. Soc.* **1990**, *112*, 3579–3583. (h) Ostovic, D.; Lee, I. S. H.; Roberts, R. M. G.; Kreevoy, M. M. *J. Org. Chem.* **1985**, *50*, 4206–4211.

(36) (a) Aizpurua, J. M.; Palomo, C.; Fratila, R. M.; Ferron, P.; Benito, A.; Gomez-Bengoa, E.; Miranda, J. I.; Santos, J. I. *J. Org. Chem.* **2009**, *74*, 6691–6702. (b) Hapiot, P.; Moiroux, J.; Saveant, J. M. *J. Am. Chem. Soc.* **1990**, *112*, 1337–1343. (c) Xu, H.-J.; Dai, D.-M.; Liu, Y.-C.; Li, J.; Luo, S.-W.; Wu, Y.-D. *Tetrahedron Lett.* **2005**, *46*, 5739–5742. (d) Ellis, W. W.; Raebiger, J. W.; Curtis, C. J.; Bruno, J. W.; DuBois, D. L. *J. Am. Chem. Soc.* **2004**, *126*, 2738–2743.

(37) (a) Ogata, K.; Murayama, H.; Sugasawa, J.; Suzuki, N.; Fukuzawa, S.-i. *J. Am. Chem. Soc.* **2009**, *131*, 3176–3177. (b) Srogl, J.; Voltrova, S. *Org. Lett.* **2009**, *11*, 843–845. (c) Dzygiel, P.; Reeve, T. B.; Piarulli, U.; Krupicka, M.; Tvaroska, I.; Gennari, C. *Eur. J. Org. Chem.* **2008**, *No. 7*, 1253–1264. (d) Sharma, R. K.; Nethaji, M.; Samuelson, A. G. *Tetrahedron: Asym.* **2008**, *19*, 655–663. (e) Ram, R. N.; Singh, V. *Tetrahedron Lett.* **2006**, *47*, 7625–7628.

(38) (a) Xu, H.-J.; Liu, Y.-C.; Fu, Y.; Wu, Y.-D. *Org. Lett.* **2006**, *8*, 3449–3451. (b) Lo, H. C.; Fish, R. H. *Angew. Chem., Int. Ed.* **2002**, *41*, 478–481.

(39) (a) Fang, X. Q.; Xu, H. J.; Jiang, H.; Liu, Y. C.; Fu, Y.; Wu, Y. D. *Tetrahedron Lett.* **2009**, *50*, 312–315. (b) Akagawa, K.; Akabane, H.; Sakamoto, S.; Kudo, K. *Org. Lett.* **2008**, *10*, 2035–2037. (c) Kang, Q.; Zhao, Z.-A.; You, S.-L. *Org. Lett.* **2008**, *10*, 2031–2034. (d) Martin, N. J. A.; Ozores, L.; List, B. *J. Am. Chem. Soc.* **2007**, *129*, 8976–8977. (e) Yang, J. W.; List, B. *Org. Lett.* **2006**, *8*, 5653–5655. (f) Martin, N. J. A.; List, B. *J. Am. Chem. Soc.* **2006**, *128*, 13368–13369. (g) Zhang, Z.; Gao, J.; Xia, J.-J.; Wang, G.-W. *Org. Biomol. Chem.* **2005**, *3*, 1617–1619.

(40) (a) Fukuzumi, S.; Suenobu, T.; Kawamura, S.; Ishida, A.; Mikami, K. *Chem. Commun.* **1997**, *No. 3*, 291–292. (b) Fukuzumi, S.; Tokuda, Y. *Bull. Chem. Soc. Jpn.* **1992**, *65*, 831–836.

(41) Chikashita, H.; Ide, H.; Itoh, K. *J. Org. Chem.* **1986**, *51*, 5400–5405.

(42) Sigala, P. A.; Kraut, D. A.; Caaveiro, J. M. M.; Pybus, B.; Ruben, E. A.; Ringe, D.; Petsko, G. A.; Herschlag, D. *J. Am. Chem. Soc.* **2008**, *130*, 13696–13708.

(43) (a) Zhang, B.-L.; Zhu, X.-Q.; Lu, J.-Y.; He, J.-Q.; Wang, P. G.; Cheng, J.-P. *J. Org. Chem.* **2003**, *68*, 3295–3298. (b) Zhu, X.-Q.; Wang, H.-Y.; Wang, J.-S.; Liu, Y.-C. *J. Org. Chem.* **2001**, *66*, 344–347.

(44) Kimura, M.; Tanaka, K. *Angew. Chem., Int. Ed.* **2008**, *47*, 9768–9771.

(45) Ohno, A.; Oda, S.; Ishikawa, Y.; Yamazaki, N. *J. Org. Chem.* **2000**, *65*, 6381–6387.

(46) Isaacs, N. S. *Physical Organic Chemistry*, 2nd ed.; Addison Wesley Longman: London, 1995.

(47) Cho, B. H.; Kim, J. H.; Jeon, H. B.; Kim, K. S. *Tetrahedron* **2005**, *61*, 4341–4346.

(48) Viscontini, M.; Hochreuter, R.; Karrer, P. *Helv. Chim. Acta* **1953**, *36*, 1777–1783.

(49) Dauben, J. H.; Honnen, L.; Harmon, K. *J. Org. Chem.* **1960**, *25*, 1442–1445.

(50) Zhu, X.-Q.; Zhang, M.-T.; Yu, A.; Wang, C.-H.; Cheng, J.-P. *J. Am. Chem. Soc.* **2008**, *130*, 2501–2516.

(51) Zhu, X.-Q.; Liang, H.; Zhu, Y.; Cheng, J.-P. *J. Org. Chem.* **2008**, *73*, 8403–8410.

(52) Zhu, X.-Q.; Tan, Y.; Cao, C.-T. *J. Phys. Chem. B* **2010**, *114*, 2058–2075.

(53) Equations 5−7 were constructed from the thermodynamic cycles in Scheme 4. Note that we used the term free-energy change ΔG_{et} to replace the enthalpy change ΔH_{et} in eqs 5−7 for the electron transfer processes. The justification of this treatment is that entropies associated with electron transfer are negligible, as verified by Arnett et al: Arnett, E. M.; Amarnath, K.; Harvey, N. G.; Cheng, J.-P. *J. Am. Chem. Soc.* **1990**, *112*, 344–355.

(54) Wayner, D. D. M.; Parker, V. D. *Acc. Chem. Res.* **1993**, *26*, 287–294.

(55) Zhang, X.-M.; Bruno, J. W.; Enynnaya, E. *J. Org. Chem.* **1998**, *63*, 4671.

(56) Warren, J. J.; Tronic, T. A.; Mayer, J. M. *Chem. Rev.* **2010**, *110*, 6961–7001.

(57) Miller, L. L.; Valentine, J. R. *J. Am. Chem. Soc.* **1988**, *110*, 3982–3989.

(58) Zhu, X.-Q.; Liu, Q.-Y.; Chen, Q.; Mei, L.-R. *J. Org. Chem.* **2010**, *75*, 789–808.

(59) (a) Page, M.; Williams, A. *Organic and Bio-organic Mechanism*; Longman: Harlow, UK, 1997; Chapter 3, pp 52−79. (b) Williams, A. *Acc. Chem. Res.* **1984**, *17*, 425–430. (c) Williams, A. *Acc. Chem. Res.* **1989**, *22*, 387–392. (d) Williams, A. *Adv. Phys. Org. Chem.* **1991**, *27*, 1. (e) Williams, A. *J. Am. Chem. Soc.* **1985**, *107*, 6335–6339.

(60) Eberson, L. *Electron Transfer Reactions in Organic Chemistry*; Springer: Berlin, 1987.

(61) (a) Marcus, R. A. *J. Phys. Chem.* **1968**, *72*, 891–899. (b) Albery, W. J. *Annu. Rev. Phys. Chem.* **1980**, *31*, 227–263. (c) Breugst, M.; Zipse, H.; Guthrie, J. P.; Mayr, H. *Angew. Chem., Int. Ed.* **2010**, *49*, 5165–5169.

(62) According to Hammett equation $\log K = \rho\sigma$ and $\Delta H \approx -RT \log K$, the line slope of ΔH against σ should be approximately equal to -5.7ρ.

(63) Zhu, X.-Q.; Li, Q.; Hao, W.-F.; Cheng, J.-P. *J. Am. Chem. Soc.* **2002**, *124*, 9887–9893.

(64) The value is derived from the *k*-value of C_{sp^3}−H in gas (674.6 kcal Å^2 mol^{-1} from the following book: Cottrell, T. L. *The strengths of Chemical Bonds*; Butterworths Scientific Publication: London, 1954)

after revision by using solvent (acetonitrile) effect on the C_{sp^3}—H bond dissociation energy.

(65) Typically, the first injection shows less heat than expected. This is often due to diffusion across the tip of the needle or to difficulties in positioning the buret drive.